NASA Technical Paper 1843

A Diagnostic Model for Studying Daytime Urban Air-Quality Trends

Dana A. Brewer, Ellis E. Remsberg,
and Gerard E. Woodbury

MAY 1981

NASA

NASA Technical Paper 1843

A Diagnostic Model for Studying Daytime Urban Air-Quality Trends

Dana A. Brewer
The George Washington University
Joint Institute for Advancement of Flight Sciences
Langley Research Center
Hampton, Virginia

Ellis E. Remsberg and Gerard E. Woodbury
Langley Research Center
Hampton, Virginia

National Aeronautics
and Space Administration

**Scientific and Technical
Information Branch**

1981

SUMMARY

A single-cell Eulerian photochemical air-quality simulation model was developed and validated for selected days of the 1976 St. Louis Regional Air Pollution Study (RAPS) data sets; parameterizations of variables in the model and validation studies using the model are discussed. Good agreement was obtained between measured and modeled concentrations of NO, CO, and NO_2 for all days simulated. The maximum concentration of O_3 was also predicted well. Predicted species concentrations were relatively insensitive to small variations in CO and NO_x emissions and to the concentrations of species which are entrained as the mixed layer rises. Because of the rather small horizontal dimensions of the single cell (20 km by 20 km), predicted species concentrations were sensitive to the advection of upwind ozone and its precursors. Chemical reactions were dominated by the chemistry of reactive hydrocarbons. Significant changes in the predicted concentrations of O_3 were also obtained when photolytic reaction rates were scaled from theoretical to atmospheric values to reflect the attenuation of solar radiation by particulates and aerosols. The uses of additional types of data in the model formulation and validation procedures are discussed.

INTRODUCTION

The NASA Langley Research Center has programs to develop both in situ and remote sensors for environmental air-quality measurements on the regional to global scale. Initial testing of the sensors normally occurs over relatively small (local) spatial scales using several instrumented aircraft available at Wallops Flight Center, Jet Propulsion Laboratory, and Langley Research Center. From 1977 to 1979, a series of summer field-measurement programs, the Southeastern Virginia Urban Plume Studies (SEV-UPS), were performed to evaluate several NASA remote sensors (refs. 1 and 2). To assist in the interpretation of these measurements, an urban-scale air-quality simulation model was developed.

The model utilizes a single-volume element or cell centered over an urban area with a fixed horizontal length and a variable vertical height that depends on the height of the mixed layer. Transport through the cell and photochemistry within the cell are treated simultaneously. The present paper describes the validation of this model by using several data sets obtained during the 1976 EPA Regional Air Pollution Study (RAPS) in St. Louis (ref. 3).

The general approach used in the single-cell air-quality model of Schere and Demerjian (ref. 4) was followed in the present study. The representation of the physical processes in the single-cell model is compatible with the type and quantity of data that are normally present in urban air-quality and emissions data bases. An Eulerian photochemical air-quality simulation model similar to the model developed by Schere and Demerjian was developed and tested by comparing the model results with measurements from selected days in the RAPS

data set. When the methods used to parameterize variables in the Schere and Demerjian model (ref. 4) were defined, those methods were also used to parameterize this model. However, the parameterizations for several key variables were not described in sufficient detail for inclusion in this model. The variables which were parameterized in this study, and consequently differ from Schere and Demerjian's model (ref. 4), are as follows: chemical mechanism, emissions inventory, growth rate of the mixed layer, and background and entrainment concentrations. The chemical mechanism describes only gaseous chemical reactions. The model is applicable principally to clear-sky days; however, days with cloudy skies can be modeled if solar radiation measurements are available. The justifications for using the present modified techniques and input parameters are discussed in the subsequent sections. As a result, the verification results of air-quality trends for St. Louis for July 23, 1976 (day 205), and August 3, 1976 (day 216), two days presented by Schere and Demerjian, are necessarily somewhat different from results presented previously by those authors. In addition, verification studies using additional clear-sky days in the RAPS data set, June 7, June 8, July 13, and August 13, 1976 (days 159, 160, 195, and 226, respectively), are discussed. Day numbers instead of dates are used throughout the present paper.

MATHEMATICAL MODELING APPROACH

The basic working equations governing the prediction of species concentrations for the single cell model are as follows:

$$\frac{\partial c_{i,t}}{\partial t} = \frac{\bar{Q}_i}{z_t} + \frac{\bar{U}}{\Delta x}(c_{i,bg} - c_{i,t-1}) + \left(\frac{z_t - z_{t-1}}{z_t\,\Delta t}\right)(c_{i,top} - c_{i,t-1}) + R_i \qquad (1)$$

$$c_{i,t} = \int_{t-1}^{t} \frac{\partial c_{i,t}}{\partial t}\,dt \qquad (2)$$

where

$c_{i,t}$ concentration of species i at time t, ppmv-hr^{-1}

$\bar{Q}_i$ hourly averaged emissions flux of species i, ppmv-m-hr^{-1}

z_t height of mixing layer at time t, m

$c_{i,bg}$ concentration of species i at time t-1 upwind of the modeling region, ppmv

$c_{i,top}$ concentration of species i above the mixing layer, ppmv

Δx horizontal length of cell, km

$\bar{U}$ hourly averaged wind speed through cell, $m\text{-}hr^{-1}$

R_i differential rate of change of species concentrations due to chemical reactions, $ppmv\text{-}hr^{-1}$

t time

Δt time increment, hr

The transport and chemistry of the atmospheric species are coupled in order to better simulate the air quality in an urban area as seen by the in situ sensors. The time rate of change of species concentrations as predicted by equation (1) is dependent upon each of the following terms on the right-hand side: emissions into the cell, the advection inflow through the cell, the dilution effect of the expanding volume of the cell as the mixed layer rises, the entrainment of any pollutant species aloft, and the production and/or destruction of species caused by chemical reactions within the volume. Dry deposition and surface scavenging are neglected because insufficient data exist to parameterize or validate these processes. Figure 1 shows the cell centered over St. Louis with a horizontal cell length x of 20 km. The Regional Air Monitoring (RAM) station locations used to obtain the RAPS data set (ref. 3) are indicated.

The horizontal lengths of the cell are fixed in the beginning of the modeling period, the base of the cell is the ground, and the top of the cell is the mixing layer height, which normally increases during daylight hours. Turbulent mixing, which produces uniform species concentrations within the cell volume is assumed to occur; therefore, diffusion is neglected. The geographic position of the cell, which is arbitrarily defined, is constant throughout the simulation. The direction of advection through the cell is defined by the prevailing wind direction and, therefore, any change slightly during the simulation. Thus, horizontal fluxes through the model cell may not always enter the cell perpendicular to a cell face.

Chemical species were separated into three groups based on the chemical lifetimes. The separation into groups was performed to reduce the order of the matrix that was integrated and thus reduce the time required for integration (ref. 5). Concentrations of species in two groups were held constant while solutions for species concentrations in a third group were obtained.

Group 1 contains species whose lifetimes of several days are much greater than the time step (1.5 minutes) for integration of species concentrations. Species in the group (which include CO_2, H_2O, O_2, and inert gases) have low chemical reactivities. Concentrations of these species were held constant throughout the simulation.

Group 2 contains species whose chemical lifetimes are several hours in length; diurnal variations in concentrations are routinely monitored. Species defined by the Environmental Protection Agency (ref. 6) as criteria pollutants (NO_2, NO, O_3, and CO) and other stable compounds are members of the group. Chemical reactions couple species concentrations within this group to species

concentrations both within and outside of the group. Integration of the equations describing the changes in concentrations $\delta c_i/\delta t$ is performed using the EPISODE algorithm (ref. 7).

Group 3 contains species whose lifetimes are short, on the order of seconds or a few minutes. The species have low concentrations and high chemical reactivities and include reaction intermediates and radicals such as OH, HO_2, NO_3, and RCO_3. The equations describing the concentration changes of species in the group reduce from differential to nonlinear algebraic form when the steady-state hypothesis ($\delta c_i/\delta t = 0$) is invoked. As a consequence of using the steady-state hypothesis, transport is neglected for species in this group. Since the algebraic equations are coupled, they are solved iteratively until a stable solution for all group 3 species concentrations is achieved.

The sequence of computations used to obtain predicted species concentrations is as follows. Measured concentrations of the coupled species at 0530 local standard time (LST) were used to calculate concentrations of the steady-state species (group 3) at 0530 LST. The complete set of species concentrations was then used to form differential expressions (eq. (1)) for each of the coupled species. Concentrations of coupled species returned from EPISODE for the subsequent time step were then used as constants in the solution of steady-state species concentrations for the subsequent time step. The sequence of computations was repeated for the remainder of the simulations.

PHOTOCHEMICAL MECHANISM

The Falls and Seinfeld mechanism (ref. 8) was used in this model to describe the chemical kinetics that occur in the urban troposphere. The mechanism describes the gaseous chemical reactions of ozone, nitrogen oxides, and hydrocarbons in an urban atmosphere. Heterogeneous chemistry is not treated. Rate constants for thermal reactions were adjusted hourly using Arrhenius kinetics to account for the diurnal temperature variations.

Hydrocarbons in the mechanism are partitioned into classes based on bonding characteristics; that is, hydrocarbons are separated into alkanes, ethylene, other alkenes, formaldehyde, other aldehydes, organic nitrates, and alkoxy and alkyl peroxy radicals. Hydrocarbon chemistry generally dominates the prediction of diurnal concentrations of ozone in urban atmospheres. However, the RAPS data set does not include speciation of nonmethane hydrocarbons, which is a requirement for the efficient utilization of the mechanism. The sensitivity of the mechanism to variations in nonmethane hydrocarbon concentrations is addressed in a subsequent section.

Quantum yields for the photolysis of NO_2 in the laboratory were obtained from Jones and Bayes (ref. 9) and used as input in an algorithm developed by Schere and Demerjian (ref. 10) to compute diurnal variations of all photolytic rate constants in the mechanism. The theoretical rate constants are computed for clear-sky conditions and are a function of actinic flux, date, time, and location of the modeled region. Photolytic rate constants in the atmosphere are reduced relative to their theoretical values because of the attenuation of solar radiation by aerosols and gases in the polluted atmosphere; Zafonte

et al. (ref. 11) parameterized the attenuation by introducing a zenith-angle dependence into the atmospheric value of the photolytic rate constant for NO_2. The rate constant for the photolysis of NO_2 used in this calculation k_{NO_2} was reduced relative to its theoretical value by using an empirical scaling factor parameterized for the St. Louis area by Schere and Demerjian (ref. 4) and based on the work of Zafonte et al. (ref. 11). The scaling factor is a function of the measured (UV to near-IR) total solar radiation (TSR), the solar zenith angle z, and the theoretical photolysis rate for NO_2:

$$k_{NO_2}(\text{scaled}) = [-0.0696 + 0.835(1 - \cos z)](\text{TSR}) \qquad (64^\circ \leq z < 90^\circ)$$

$$k_{NO_2}(\text{scaled}) = 0.4064(\text{TSR}) \qquad (47^\circ \leq z < 64^\circ)$$

$$k_{NO_2}(\text{scaled}) = \left[0.295 + 0.076\left(\frac{1}{\cos z}\right)\right](\text{TSR}) \qquad (0^\circ \leq z < 47^\circ)$$

Rate constants for other photolytic reactions in the mechanism were reduced by a scale factor of $k_{NO_2}(\text{scaled})/k_{NO_2}(\text{theoretical})$. The days chosen for simulations in this work were primarily clear-sky days; thus, smooth variations in the photolytic rate constants were obtained.

SPECIES CONCENTRATIONS

The rationale for selecting concentrations of species required to integrate equation (1) is discussed in this section.

Concentrations of O_3, CH_4, NO, NO_2, and total hydrocarbons were measured at many stations within and surrounding the urban area shown in figure 1 (ref. 3). An hourly averaged concentration for each species was calculated by using measurements at all stations within the cell for a given hour. Average measured concentrations for 0530 LST, the starting time for simulations, were used to initialize the model. Average measured concentrations for later hours were compared with calculated concentrations.

Methane and total hydrocarbon concentrations were measured in St. Louis, but since hydrogen speciation was not part of the archived RAPS data set, partitioning of nonmethane hydrocarbons into bonding classes present in the mechanism (ref. 8) was performed within the model. The partitioning process was based on the relative percentages of average ambient concentrations of hydrocarbons measured in Los Angeles in 1965 (ref. 12). Table I shows the levels and percentages of hydrocarbons found in Los Angeles in 1965 along with scale factors and percentages of hydrocarbons used in the present study. The percentages of reactive hydrocarbons found in St. Louis were expected to be substantially less than those in Los Angeles. The scale factors used for all final simulations, which were varied in increments of 5 percent for each nonmethane hydrocarbon class, were determined by modeling days 205 and 216 simultaneously in order to obtain calculated ozone curves which agreed in both magnitude and shape with the measured curves. Meteorological conditions and ozone air-quality trends for days 205 and 216 were markedly different from each other; simultaneous attempts

to match the ozone for both days resulted in hydrocarbon scaling factors that were more general than those which would have been obtained if each day had been considered separately. The effect of varying the scale factors on the prediction of the magnitude of the ozone concentration for day 216 is shown in figure 2. Note that the hours are denoted by 5, 7, etc., instead of 0500, 0700, etc. The measured ozone concentration is denoted by circles; the shaded area represents a range of one standard deviation about the mean for ozone concentrations measured at all stations within the model cell at each hour. A change in the scale factors had no effect on the computed CO curve and only minor effects on the computed NO and NO_2 curves. While the scale factors used in this study are not definitive for the St. Louis study, they provided the best agreement of modeled and measured results for the days simulated and for the scale factors considered. More recent measurements of hydrocarbon speciation in major U.S. cities (including St. Louis) show reactive hydrocarbon partitioning coefficients which are quite similar to those used in this model (ref. 13).

Nonzero concentrations for all species are required to initiate the chemical-reaction portion of the model. Initial concentrations of species not measured but included in the mechanism were estimated by using the values of Duewer (ref. 14) when available. When not measured or available from Duewer, initial species concentrations inside the cell were set equal to the concentrations upwind of the cell $c_{i,bg}$. (See table II.)

Wind-direction measurements were used to select stations that measured hourly concentrations of coupled species upwind of the cell $c_{i,bg}$. An axis system containing 45° arcs was centered over the modeling region. The midpoints of the arcs correspond to $N(0^{\circ})$, $NE(45^{\circ})$, $E(90^{\circ})$, etc. Stations were selected when their locations corresponded to the measured wind direction.

Measurements of upwind concentrations of coupled species were not available for all hours simulated. Since hourly nonzero values are required to describe the transport through the cell, a sensitivity study was devised to estimate upwind concentrations. Measured initial concentrations inside the cell, upwind concentrations, concentration estimates from Duewer (ref. 14), and first-guess concentrations for coupled species were used to simulate diurnal concentrations for days 205 and 216. The first-guess concentrations were then successively varied, one species at a time, and the effects of a single concentration variation on the simulated concentrations of O_3, NO, NO_2, and CO for days 205 and 216 were examined. Unknown species concentrations (such as aldehydes) were reduced to the point where small variations in concentrations had no effect on computed ozone concentrations.

An example of the effects of varying first-guess concentrations on the computed ozone concentrations for day 216 is shown in figure 3. All concentrations except those being varied are equal to the values listed in table II. In figure 3(a), modeled values are shown for two cases, one (the upper curve) where the initial and upwind concentrations of formaldehyde and of the group "other aldehydes" were each equal to 10 ppb and the other (the lower modeled curve) where the concentrations of both species were equal to 0.5 ppb. The latter concentrations were used to simulate all the days in this study. Figure 3(b) shows the effects of changing only the HNO_2 and RNO_2 concentrations from the initial

estimates of 10 ppb to the concentrations of 0.1 ppb which were used in this study and are given in table II.

Measurements of concentrations of coupled species above the mixed layer $c_{i,top}$ were not available; the concentrations were estimated (table II) and, with the exception of ozone, were held constant for all hours and days simulated. Estimates of other species concentrations above the mixed layer were obtained from Duewer (ref. 14) when available and made independently when not available. Ozone received separate treatment from other species since higher ozone concentrations above the mixed layer may occur during air stagnation periods. When a subsidence inversion existed on a day being simulated, as was the case for day 205, the concentration of ozone above the mixed layer, the entrained concentration, was increased from its prescribed value of 0.025 ppm (ref. 14) to a higher value which was determined from the magnitude of the measured ozone curve for the previous day and from the diurnal variation in meteorological conditions. Previous studies (ref. 15) showed that the computed maximum ozone concentration in this model is relatively insensitive to the entrained ozone concentration $c_{i,top}$ when ozone concentrations are measured at upwind stations. The rate of change of ozone concentration within the cell is influenced more by ozone advected into the cell than by vertical mixing. Upwind ozone advected into the cell, which is obtained from hourly measurements, includes a contribution from entrained ozone.

The RAPS data set included hourly averaged values for anthropogenic area and point-source emissions, $\bar{Q}$ in equation (1). Since emissions were defined in terms of a somewhat smaller grid than the cell size, the smaller grids were summed to obtain hourly emissions in the modeling region. Using measured minimum and maximum mixing-layer heights as input, appropriate plume-rise algorithms (refs. 16 and 17) were applied to hourly point-source emissions to account for emissions which might escape above the mixed layer. For the most part, the net effect of the plume-rise algorithms was to reduce emissions where low mixing heights were present.

Emissions classes in the RAPS data set are nitrogen oxides (NOX), total hydrocarbons (THC), CO, nonreactive hydrocarbons, paraffins, total olefins, aromatics, and total aldehydes. Diurnal variations in the emissions of CO, NOX, and the reactive hydrocarbons (the sum of paraffins, olefins, aromatics, and aldehydes) are shown in figure 4. Based on emissions data for Los Angeles (ref. 12), emissions classes were partitioned into 90 percent NO and 10 percent NO_2; total aldehydes were divided into 66 percent formaldehyde and 34 percent other aldehydes; and total olefins were partitioned into 59 percent ethylene and 41 percent other olefins. While the partitioning coefficients for St. Louis emissions may not have the same absolute percentages as those for Los Angeles, previous studies (ref. 15) show that small changes in emissions have little effect on simulated species concentrations.

Using the RAPS emissions inventory (version available in Feb. 1980), emissions were compiled for days 205 (Friday) and 216 (Tuesday). It was assumed that those weekday emissions were typical values for all summer weekdays since predicted oxidant levels were shown to be relatively insensitive to small variations in CO and NO_x emissions (ref. 15). Therefore, emissions for day 216 were

also used to simulate day 226 (Friday), and emissions for day 205 were used to simulate days 159 (Monday), 160 (Tuesday), and 195 (Tuesday).

METEOROLOGY

Meteorological data were measured at the surface at most RAM stations; the measurements used in the model were wind speed, wind direction, temperature, dew point, barometric pressure, and solar insolation. A single hourly averaged value for each parameter was formed using all stations within the cell (fig. 1). Wind speed and wind direction were used in two ways: to define transport through the cell using equation (1), and to determine which stations upwind of the cell were used to specify concentrations $c_{i,bg}$ advected into the cell. Dew-point measurements determined appropriate concentrations of water vapor. Temperature and barometric pressure measurements were used to maintain conservation of mass in the model. Solar insolation was used to calculate UV-scaled photolytic rate constants.

The height of the mixed layer characteristically increases during daylight hours (ref. 18), and the calculations are very sensitive to this growth parameter. The rate of growth per hour varies with the time of day, with solar insolation, and with the larger-scale synoptic conditions. The minimum and maximum heights of the mixed layer vary with the day being simulated. Mixing heights were measured by the RAPS Upper Air Sounding Network (ref. 3) at only one station inside the cell, station 141, and at 6-hour intervals - approximately 0400, 1000, 1600, and 2200 LST (table III). Measurements made at 0400 and 1600 LST established the minimum and maximum heights of the mixed layer, respectively; measurements made at 1000 LST were used as guidelines for establishing the percentage growth for the rise of the mixed layer from the minimum value to a value at 1030 LST. For the 0400 LST mixing-height measurement for 5 of the 6 days in table III, the mixing depth as defined in the archived data tapes is listed as zero. This is due to the presence of a surface nocturnal inversion (ref. 19). In all five situations, however, a second low-level stable layer was present, and later in the morning it was eroded because of surface heating. In order to allow for a finite modeling volume at the start of a daily calculation, the top of the cell was set as the base of the elevated stable layer, even though it is not clear whether materials injected into the volume in the morning hours are mixed up to that base level. Knowledge of how quickly the low-level stable layer actually eroded would be helpful, but continuous measurements of the boundary-layer structure are needed for such an assessment.

CO is used as an indicator of the growth rate of the mixed layer since changes in CO concentrations are derived primarily from volume changes within the cell and from transport through the cell rather than from chemical reactions (assuming that the emissions inventory adequately describes CO sources in the cell). When continuous measurements of the mixing-layer height are not available, good agreement between measured and simulated CO concentrations can be obtained by adjusting the growth function for the rise of the mixed layer. This technique was used in model studies of the San Francisco Bay area using the Livermore Regional Air Quality (LIRAQ) model (ref. 20). Using this approach, the early morning measured CO "traffic" peak was reproduced reasonably. Percentage differences between the measured and modeled rates of growth are shown

in the last two columns of table III, and for two (195 and 205) of the 6 days (159, 160, 195, 205, 216, and 226), those differences were appreciable. The vertical temperature-gradient data near the ground indicated a strong surface inversion on the morning of day 205. For the remaining day (195), there was no early morning surface inversion, and the related meteorological parameters as well as the surface CO and NO air-quality data indicate good advection and surface heating in the morning. Surprisingly, however, the measured mixing height rose only 110 m (from 384 m to 494 m) from 0349 LST to 1048 LST, although it eventually grew to a level of 1905 m at 1550 LST. The mixing height of 494 m at 1048 LST, if accurate, is therefore judged to have been ineffective in capping the volume, and this would explain the large discrepancy between the measured and adjusted percentage growth rates for day 195. Therefore, when the discrepancies in the measured mixing heights for days 195 and 205 are considered, the estimated rates of growth of the mixed layer agree well with the measured growth rates.

As indicated in the preceding discussion, the variation of CO with time is used as an indicator of the growth of the cell volume due to the mixing-height rise of the transport and of the emissions components of the model. Only one chemical reaction involving CO,

$$CO + OH \xrightarrow{O_2} CO_2 + HO_2$$

occurs in the model, and it is of minor importance to the urban photochemistry. Since diffusion is neglected and only one-dimensional horizontal transport is considered in this model, the diurnal variation of CO concentration then becomes a good indicator of transport through the cell. The primary urban source of CO is vehicle emissions. If CO concentrations were dominated by vehicle emissions, then diurnal CO concentrations should closely follow fluctuations in traffic density. In particular, a 1- to 2-hour peak concentration should occur in the early morning followed by a gradual decrease in CO concentration (ref. 21). However, a sharp rather than a broad CO peak occurs in the measurements early in the morning, which reflects the beginning of the rise of the mixed layer, and thus the dilution of the CO concentration due to the expanding volume of the cell.

In general, CO measurements are obtained at the surface close to the source emissions and, since CO concentrations are source dependent, They are spatially quite inhomogeneous. Likewise, vertical CO concentrations should be quite inhomogeneous and should decrease with altitude, especially during stable atmospheric situations. Simulations predict CO concentrations only for the middle of the cell volume. Modeled CO concentrations should then be somewhat lower than measured concentrations.

The starting times for the rapid growth of the mixed layer were determined by noting the times of the morning maxima in the CO curves. The CO peaks, and thus the starting times for rapid growth, occurred between 0630 and 0730 LST and depended upon the particular day being simulated. Table IV shows the hourly growth rate of the mixed layer used in the model.

The surface heating during the sunlight hours retains the base of the mixed layer at the surface. At sunset, the base of the mixed layer is no longer constrained to the surface, and, in fact, may form a mixed layer aloft. Clean air then enters beneath the mixed layer, which produces discontinuities in surface concentration measurements. Since this physical process is absent in this model, agreement between measured and modeled species concentrations is expected to be poor after sunset.

MODEL RESULTS AND DISCUSSION

Air quality simulations were conducted for day 205 and day 216 to gain confidence in the use of the model. Simulations for these dates were shown previously by Schere and Demerjian (ref. 4).

Figures 5(a) to (d) show the averaged measured (circles) and modeled (squares) species concentrations within the cell for day 216 for CO, NO, NO_2, and O_3, respectively. The shaded areas represent a range of one standard deviation around the mean of species concentrations measured at all stations within the cell at each hour. Moderate wind speeds, which produce good advection through the cell, existed throughout the day. The simulations show good agreement with averaged measured concentrations.

Changes in CO concentrations (fig. 5(a)) are derived primarily from volume changes in the cell, transport through the cell, and emissions inside the cell rather than from chemical reactions. For a given day, transport through the cell was determined by measurements of wind speed made at stations within the cell; it was assumed that CO sources within the cell were adequately described by the emissions inventory. Thus, the remaining variables that could be adjusted to provide better agreement between measured and simulated CO concentrations were the starting time for growth and the growth rate of the mixed layer, terms which describe volume changes in the cell.

The sharp peak in the measured morning CO concentrations is an indicator of the expanding volume of the cell and, consequently, the starting time for the growth of the mixed layer. Thus, adjustments in the growth rate were used to obtain better agreement between measured and simulated CO concentrations.

CO concentrations are source dependent with expected decreases in concentration as altitude increases. While CO measurements are made at the cell base, simulations predict concentrations in the middle of the cell volume; thus, predicted CO concentrations should be less than measured concentrations. The growth rate of the mixed layer, particularly in the morning hours, was adjusted to reflect the decrease in predicted concentrations. The increase in concentrations of all species after 1830 LST is expected. This increase is due to the breakup of the mixed layer at sunset, a process which is not described in this model.

Diurnal variations in the concentration of NO, shown in figure 5(b), result from emissions, transport, chemical reactions, and volume changes in the cell. Transport occurs throughout the day. The concentration levels of NO in the early morning, from 0530 to 0630 LST, are determined by the magnitude of the

emissions. Concentration levels of NO from 0630 to 1230 LST are dominated by emissions and increases in the cell volume; large fluctuations in the predicted concentrations of NO were obtained during this time period when the growth rate of the mixed layer and the emissions flux of NO were varied. After 1230 LST, variations in the emissions flux and growth rate of the mixed layer had negligible effects on the concentration levels of NO, which indicated that chemical reactions dominated the levels of predicted species concentrations. Emissions of NO generally occur close to the ground, and measurements of species concentrations are made at the ground; species concentrations are calculated for the middle of the cell volume. It is assumed that uniform mixing occurs in the model; however, when emissions are large, as they are in the early morning, instantaneous mixing of the emissions throughout the cell volume may not actually occur. Therefore, when emissions are important contributors to the concentrations of NO in the cell, from 0530 to 1230 LST, predicted NO concentrations should be and are greater than measured concentrations.

Two observations concerning the NO curves were made during the model validation process and are worth noting. First, a more rapid decrease in NO concentrations from 0630 to 1230 (obtained by increasing the growth rate of the mixed layer) increases the maximum ozone concentration predicted for the day. A probable explanation for this observation is that NO scavenges ozone through the reaction

$$O_3 + NO \rightarrow NO_2 + O_2$$

Therefore, increased NO concentrations inhibit production of ozone. Secondly, the maximum ozone concentration occurs 4 to 5 hours after the crossing of the measured and modeled NO curves (at 1230 LST). The crossing (and thus the time of occurrence of the maximum ozone concentration) can be changed slightly by adjusting the growth rate of the mixed layer.

The diurnal variations in the concentration of NO_2, shown in figure 5(c), result from emissions, transport, chemical reactions, and volume changes in the cell. It is not clear from examining the fluctuations in the averages of measurements made inside the cell whether a single process dominates at any given time. The shape of the simulated curve and the magnitudes of simulated NO_2 concentrations should agree with those obtained from measurements in order to obtain good agreement between measured and modeled NO and O_3 curves.

Changes in O_3 concentrations for day 216 (fig. 5(d)) are attributed to transport and chemical reactions. Ozone is scavenged at the ground by surface reactions and dry deposition, both of which are neglected in this model. As a direct consequence, modeled ozone concentrations for afternoon hours, which represent concentrations in the middle of the cell, are expected to be greater than concentrations measured at the surface. A disparity in ozone concentrations of the order of 15 percent was observed by Duewer et al. (ref. 20) in their measured and modeled (LIRAQ) results for the San Francisco Bay area stations. The simulated O_3 concentrations obtained in this work show good agreement with average measured concentrations. The modeled ozone maximum of 121.5 ppb is 11.7 percent higher than the measured value of 108.7 ppb;

both the position of the maximum and the shape of the simulated curve agree well with the measured curve.

Predicted ozone concentrations in the morning hours (0530 to 1230 LST) are consistently lower than measured concentrations. Although it is not clear why the predicted concentrations are underestimated, one possible explanation is that the chemical mechanism overcompensates for ozone scavenging by NO. This discrepancy also appears in simulations of other days and certainly warrants study in the future.

An inversion existed on day 205 (simulations shown in fig. 6) which provided quite different meteorology from day 216. Ozone from the previous day was trapped aloft since the wind speeds were insufficient to introduce clean air above the urban area. Consequently, an elevated entrainment concentration of 60 ppb ozone was used (ref. 4). Since previous studies (ref. 15) showed that the model results are relatively insensitive to the concentration of ozone aloft when measured concentrations at stations upwind of the cell are available, the entrainment concentration of 60 ppb for day 205 compared with the "clean air" value of 25 ppb indicates only the existence of an inversion but not necessarily the exact strength of the inversion. The measured morning growth rate for the rise of the mixed layer was less than the growth rate for day 216. The estimated morning growth rate for day 205 was similarly reduced relative to day 216 in order to decrease the computed maximum ozone concentration and increase the width of the computed ozone-concentration curve. The computed ozone maximum had a value 13.7 percent higher (94.5 ppb) than the measured ozone concentration (83.1 ppb).

Simulations for days 205 and 216 were performed to parameterize the partitioning coefficients for total hydrocarbon concentrations into hydrocarbon species and to determine appropriate initial concentrations of other species; verifications of the parameterizations were obtained through additional simulations of days 159, 160, 195, and 226. A critical variable in the simulations was the growth rate of the mixed layer. When days 159, 160, 195, and 226 were simulated, modeled CO concentrations were larger than measured concentrations throughout the day, which suggests that representative CO emissions were too large in the early morning. The introduction of a small early morning growth rate (less than 2.5 percent per hour) prior to the morning peak in the measured CO curve allowed modeled CO concentrations to remain lower than measured results throughout the day.

Simulations for day 160 are shown in figure 7. The vertical temperature gradient measured between the surface and the top of a 30-m tower was negative, which indicated that no inversion was present. Ozone reached a maximum measured concentration (averaged over all stations inside the cell) of 124.5 ppb on the previous day. The measured concentrations of CO, NO, and NO_2 in the morning hours were much higher than the morning concentrations of those species on previous days (days 205 and 216); in fact, the measured average concentration of NO at 0530 LST, the starting time for the simulation, was about three times as large as initial NO concentrations for days 205 and 216. The increased initial concentrations for this day could introduce difficulties in the simulation, since the model was validated using the lower concentrations of days 205 and 216. A distinct morning peak in the measured CO and NO concentrations (which indi-

cates the starting time for the growth of the mixed layer) was not evident. Although fairly large increases in the concentration for this day were present, no difficulties were encountered in simulating concentrations. Good agreement with the measured concentrations was obtained in the simulations of CO, NO, and NO_2. The maximum in modeled ozone concentrations of 174 ppb also compared quite favorably with the measured maximum concentration of 163 ppb (a difference of 7 percent).

Figure 8 shows simulations for day 195. Moderate wind speeds measured for for this day provided good advection through the cell. Initial concentrations of CO, NO, and NO_2 were reduced relative to those for the validation days, but the initial concentration of ozone was at least twice as large. These variations in starting concentrations relative to the validation days provided a further test of the applicability of the model to wide ranges of concentrations. While the modeled curve for CO showed particularly good agreement with the measured CO curve in both shape and magnitude, generally good agreement was obtained between all measured and modeled curves. There was no difference in magnitude between the measured and modeled ozone-concentration maxima.

Figure 9 shows the simulations for day 159. The wind speed was very low, and the measured diurnal ozone curve was broad and flat, which indicated high air pollution potential. The modeled ozone concentration reached a maximum value of 142.5 ppb at 1530 LST, which was 16.6 percent higher than the measured value of 124.5 ppb which occurred at 1330 LST. Good agreement was found between the modeled and measured concentrations of CO and NO; poorer agreement was obtained for the NO_2 curves in the morning hours. The discrepancies obtained for the NO_2 curves compared with the CO and NO curves are not surprising since a major source of NO_2 is industrial emissions but the major source of CO and NO emissions is vehicular activity. Thus, although the representative emissions used in the model may adequately represent vehicular emissions, variations in industrial emissions may account for the variations in the NO_2 curves for this day.

Maximum ozone concentrations for day 226 (fig. 10) were quite high. Cloudy sky conditions existed on the previous day with a relatively small buildup of ozone. The trailing edge of a high-pressure system was in close proximity to the simulation area. While the measured ozone curve was quite broad, adjustments in the growth rate of the mixing-layer height to produce reasonable agreement for CO, NO, and NO_2 simulations produced a narrow simulated ozone curve with a maximum concentration that was 3 percent larger than the measured peak concentration.

Table V summarizes the model performance for predicting the time of occurrence and magnitude of the ozone-concentration maxima. Modeled ozone maxima are greater than measured maxima by an average of 8.7 percent, a reasonable increase and well within the 15 percent maximum increase noted by Duewer et al. (ref. 20) in studies of the San Francisco Bay area using a more complex (LIRAQ) model. The time of occurrence of the maximum concentration of ozone was not simulated as accurately, possibly a consequence of the simplified treatment of chemistry in the model. Likewise, for all data modeled here, the predicted concentrations of ozone in the early morning hours were consistently underestimated, perhaps a consequence of overcompensating for the morning scavenging of O_3 by

NO in the chemical mechanism. The good agreement in predicting the ozone maxima and the diurnal variations in other species concentrations can be used as one criterion to assess the usefulness of the model.

The use of the model should be undertaken with some caution since the processes of dry deposition, surface scavenging, and heterogeneous reactions have not been included. Additionally, although it is assumed in the model that species concentrations are homogeneous with respect to altitude, variations in concentrations with respect to altitude have been measured for other urban areas (ref. 22). However, the model performs quite well with data from the limited number of parameters usually measured in an air-quality experiment. The addition of more detailed physics into the model to describe the urban troposphere is warranted only when data describing additional physical processes are available.

SUMMARY OF RESULTS AND CONCLUDING REMARKS

A single-cell Eulerian urban-scale air-quality simulation model was developed and validated using six clear-sky data sets obtained during the 1976 EPA Regional Air Pollution Study (RAPS) in St. Louis. The urban area is described in the model by a single cell with a fixed horizontal length and a variable vertical height which depends on the height of the mixed layer. Other parameters input to the model were wind speeds, an emissions inventory, chemical mechanism, and measured species concentrations upwind, inside, and above the cell.

Predicted species concentrations were relatively insensitive to small variations in CO and NO_x emissions and to the concentrations of species above the cell top which are entrained as the mixed layer rises. A greater sensitivity to other input parameters was shown. In particular, nonzero concentrations of species inside and upwind of the cell were required to initiate the chemical mechanism. Because of the rather small horizontal dimensions of the single cell (20 km by 20 km), predicted species concentrations were sensitive to the advection of upwind ozone and its precursors. Chemical reactions were dominated by the chemistry of the reactive hydrocarbons. Two key variables in the model had to be estimated, the coefficients used to partition emissions into species concentrations and the hourly growth rates of the mixed layer. Since chemical reaction rates are concentration dependent, simulated ozone concentrations were highly dependent upon the magnitude of the scale factor used to partition the concentrations of reactive hydrocarbons into hydrocarbon species. For 4 of the 6 days simulated in this study, the estimated growth rates of the mixed layer agreed quite well with measured values. Significant changes in the predicted concentrations of ozone were also obtained when photolytic reaction rates were scaled from theoretical to atmospheric values to reflect the attenuation of solar radiation in the atmosphere by particulates and aerosols. Information on the actual concentrations of ozone precursors and on the homogeneity in species concentrations and meteorological parameters in the modeling volume is also needed to accurately predict ozone concentrations in the middle of the cell volume.

Good agreement was obtained between measured and modeled concentrations of NO, CO, and NO_2 for all days simulated. The concentrations of ozone in the

early morning hours were consistently underestimated, a probable consequence of overcompensating for the scavenging of ozone by NO in the chemical mechanism; however, good results were obtained in predicting the magnitudes of the ozone maxima. The predicted maximum concentrations of ozone for the six simulations were an average of 8.7 percent higher than the measured maximum concentration. This is an anticipated and reasonable difference considering that the model does not treat surface scavenging and dry deposition, processes which could decrease the ozone concentrations that were measured at the ground. The most difficult data sets to simulate were those where a strong inversion was present; simulations of these data sets also showed good agreement with the measured data sets.

The model formulation could be improved if additional types of data were measured. Sufficient chemical-kinetic data are not available to include aromatic and heterogeneous chemical reactions in the chemical mechanism. Surface scavenging and dry deposition deplete measured species concentrations at the surface; measurements of the types and quantities of particles lost from dry deposition are needed. Species concentration profiles would allow for both the parameterization of the effect of surface scavenging and for the assessment of how surface scavenging and dry deposition contribute to changes in species concentrations inside the cell. Surface scavenging and dry deposition may have negligible contributions to the changes in species concentrations in the center of the cell and thus to the predictive capability of the model in the center of the cell; however, the contributions of these processes cannot be judged using the surface-station data in the RAPS data set. The parameterization of the cessation of surface heating and the subsequent formation of a mixed layer aloft would require much more information about complex meteorological processes and species concentrations. Even given the improved data set, the chemical mechanism (which was set up for daytime chemistry) would require considerable testing and perhaps modification. In any event, the parameterization is beyond the scope of the purpose of this model.

The model performance and validation could also be enhanced if several additional types of data were measured. Periodic measurements of concentrations of reactive hydrocarbon species for validation purposes and hourly measurements of the height of the mixed layer would eliminate the present need to estimate these quantities. Since transport through the center of the cell is a direct function of wind speed, the addition of vertical wind profiles rather than the use of surface winds would permit a more accurate treatment of transport through the cell. The addition of vertical concentration profiles of the criteria pollutants would give a better estimate of how well the model performs, since species concentrations are calculated in the center of the cell volume. Data in some of these areas were obtained during the RAPS field program, but none were archived for general use during the time of this work.

With the possible requirement of adding local anomalies, the model should be quite easily adapted for use in other urban centers. Measurements of species concentrations of reactive hydrocarbons are needed, and the emissions inventory, which is unique for each urban center, should be changed. Adjustments in the parameterizations for the growth of the mixed layer and for the scaling factor

for the photolysis of NO_2 are necessary. Initial species concentrations and the concentrations of background and entrained species might also require modification.

The single-cell model can be used with success when sufficient groundbased measurements are available. Since the surface-station measurements used to validate this model are of the type normally available in any large urban area from Air Pollution Control Board monitoring stations, this type of model is more readily adapted to other urban areas than more complex models requiring more detailed data sets. Still, this model requires significant amounts of data to initialize and simulate air quality for a given day. Unless accurate and periodic measurements of the height of the mixed layer are available, the model cannot fully characterize pollution episodes.

Given the limitations in the data set used for this model validation study, the present single-cell photochemical air quality model is a suitable tool for studying the chemistry and transport in an urban atmosphere.

Langley Research Center
National Aeronautics and Space Administration
Hampton, VA 23665
March 11, 1981

REFERENCES

1. Wagner, H. Scott; Gregory, Gerald L.; and Buglia, James J.: The Southeastern Virginia Urban Plume, A Test Site for Remote Sensors. Paper presented at 71st Air Pollution Control Association Annual Meeting and Exhibition (Houston, Texas), June 25-30, 1978.

2. Gregory, Gerald L.; McDougal, David S.; and Wagner, H. Scott: An Air Quality Program Designed To Evaluate Remote Sensors. NASA paper presented at the 73rd Annual Meeting Air Pollution Control Association (Place Bonaventure, Montreal, Quebec), June 22-27, 1980.

3. Strothmann, J. A.; and Schiermeier, F. A.: Documentation of the Regional Air Pollution Study (RAPS) and Related Investigations in the St. Louis Air Quality Control Region. EPA-600/4-79-076, U.S. Environ. Protection Agency, Dec. 1979. (Available from NTIS as PB80 138241.)

4. Schere, K. L.; and Demerjian, K. L.: A Photochemical Box Model for Urban Air Quality Simulation. 4th Joint Conference on Sensing of Environmental Pollutants, American Chem. Soc., c.1978, pp. 427-433.

5. Reynolds, S. D.; Ames, J.; Hecht, T. A.; Meyer, J. P.; Whitney, D. C.; and Yocke, M. A.: Continued Research in Mesoscale Air Pollution Simulation Modeling: Volume II - Refinements in the Treatment of Chemistry, Meteorology, and Numerical Integration Procedures. EPA 600/4-76-016 B, U.S. Environ. Prot. Agency, May 1976. (Available from NTIS as PB 257527.)

6. Environmental Quality - The Second Annual Report of the Council on Environmental Quality. U.S. Gov. Print. Off., Aug. 1971.

7. Hindmarsh, A. C.; and Byrne, G. D.: EPISODE: An Effective Package for the Integration of Systems of Ordinary Differential Equations. UCID-30112, Rev. 1 (Contract No. W-7405-Eng-48), Lawrence Livermore Lab., Univ. of California, Apr. 1977.

8. Falls, Andrew H.; and Seinfeld, John H.: Continued Development of a Kinetic Mechanism for Photochemical Smog. Env. Sci. & Technol., vol. 12, no. 13, 1978, pp. 1398-1406.

9. Jones, I. T. N.; and Bayes, Kyle D.: Photolysis of Nitrogen Dioxide. J. Chem. Phys., vol. 59, no. 9, Nov. 1, 1973, pp. 4836-4844.

10. Schere, Kenneth L.; and Demerjian, Kenneth L.: Calculation of Selected Photolytic Rate Constants Over a Diurnal Range - A Computer Algorithm. EPA-600/4-77-015, U.S. Environ. Prot. Agency, Mar. 1977. (Available from NTIS as PB 266739.)

11. Zafonte, Leo; Rieger, Paul L.; and Holmes, John R.: Nitrogen Dioxide Photolysis in the Los Angeles Atmosphere. Env. Sci. & Technol., vol. 11, no. 5, May 1977, pp. 483-487.

12. Heicklen, Julian: Atmospheric Chemistry. Academic Press, Inc., 1976.

13. Demerjian, Kenneth L.: The Atmospheric Photooxidation Cycle and the Influence of Troposphere Pollution on Ozone. Paper presented at the International Quadrennial Ozone Symposium (Boulder, Colorado), Aug. 4-9, 1980.

14. Duewer, William H.: Treatment of Initial and Boundary Conditions in the Application of Air Quality Models. UCID-18159 (Contr. No. W-7405-Eng-48), Lawerence Livermore Lab., Univ. of California, Apr. 1979.

15. Brewer, Dana A; and Remsberg, Ellis E.: Air Quality Model Studies With Application for Southeastern Virginia. Proceedings of Second Joint Conference on Applications of Air Pollution Meteorology and Second Conference on Industrial Meteorology, American Meteorol. Soc., Mar. 1980, pp. 61-67.

16. Briggs, Gary A.: Some Recent Analyses of Plume Rise Observation Proceedings of the Second International Clean Air Congress, H. M. Englund and W. T. Beery, eds., Academic Press, Inc., 1971, pp. 1029-1032.

17. Fay, James A.; Escudier, Marcel; and Hoult, David P.: A Correlation of Field Observations of Plume Rise. Fluid Mech. Lab. Publ. No. 69-4 (Grant No. AP 00678-01), Massachusetts Inst. Technol., Apr. 1969.

18. Tennekes, H.: A Model for the Dynamics of the Inversion Above a Convective Boundary Layer. J. Atmos. Sci., vol. 30, no. 4, May 1973, pp. 558-567.

19. Remsberg, Ellis E.; Buglia, James J.; and Woodbury, Gerard E.: The Nocturnal Inversion and Its Effect on the Dispersion of Carbon Monoxide at Ground Level in Hampton, Virginia. Atmos. Environ., vol. 13, no. 4, 1979, pp. 443-447.

20. Duewer, William H.; MacCracken, Michael C.; and Walton, John J.: The Livermore Regional Air Quality Model: II. Verification and Sample Application in the San Francisco Bay Area. J. Appl. Meteorol., vol. 17, no. 3, Mar. 1978, pp. 273-311.

21. Johnson, W. B.; Ludwig, F. L.; Dabberdt, W. F.; and Allen, R. J.: An Urban Diffusion Simulation Model for Carbon Monoxide. J. Air Pollut. Control Assoc., vol. 23, no. 6, June 1973, pp. 490-498.

22. Gregory, Gerald L.; Wornom, Dewey E.; Mathis, Joe J., Jr.; and Sebacher, Daniel I.: Summary of Aircraft Results for 1978 Southeastern Virginia Urban Plume Measurement Study of Ozone, Nitrogen Oxides, and Methane. NASA TM-80146, 1980.

TABLE I.- AVERAGE HYDROCARBON CONCENTRATION LEVELS

FOR LOS ANGELES AND ST. LOUIS

Hydrocarbon class	Los Angeles (1965)		St. Louis (present study)	
	Magnitude, ppm	THC, percent	Scale	THC, percent
Nonreactive hydrocarbons	3.22	84.99	1.1312	96.145
Alkanes	.3412	9.01	.2830	2.55
Ethylene	.06	1.58	.2278	.36
Other alkenes	.042	1.11	.2838	.315
Aromatics	.085	2.24	.2812	.63

TABLE II.- CONCENTRATIONS OF COUPLED SPECIES

Species	Concentration, ppbv*		
	$c_{initial}$	c_{bg}	c_{top}
C_2H_4	0.4	0.4	0.4
Other olefins	.4	.4	.4
H_2CO	.5	.5	.5
Other aldehydes	.5	.5	.5
O_3	†m	m	‡25.0
NO	m	m	10.0
NO_2	m	m	2.0
CO	m	m	120.0
Alkanes	35.0	35.0	35.0
HNO_2	.1	.1	.1
RNO_2	.1	.1	.1
HNO_3	1.0	1.0	1.0
RNO_3	.001	.0	.0
H_2O_2	.01	.01	.01
PAN§	.001	.0	.0

*$c_{initial}$ = Initial concentration inside the cell at 0530 LST;
c_{bg} = Background concentration, concentration upwind of cell;
c_{top} = Entrained concentration, concentration above mixed layer.
†Measured hourly.
‡For day 205, $c_{O_3,top}$ = 60.0 ppbv.
§Peroxyacetyl nitrate.

TABLE III.- DIURNAL GROWTH RATE FOR RISE OF MIXED LAYER

Day	Time, LST	Height of mixed layer, m	Base of elevated layer, m	Measured rise, percent	Modeled rise, percent
159	0345	0.	146.		
	0952	1202.	1357.	56.	56.
	1547	2046.	-----	44.	44.
160	0346	0.	146.		
	1048	2089.	-----	80.	80.
	1545	2559.	-----	20.	20.
195	0349	384.	1116.		
	1048	494.	862.	7.	75.
	1550	1905.	-----	93.	25.
205	0348	0.	223.		
	0958	1441.	-----	53.	28.
	1557	2500.	-----	47.	72.
216	0347	0.	304.		
	0948	1357.	-----	72.	64.
	1547	1767.	-----	28.	36.
226	0349	0.	176.		
	0952	1256.	1579.	85.	88.
	1547	1454.	-----	15.	12.

TABLE IV.- HOURLY GROWTH RATE OF

MIXED LAYER USED IN MODEL

Day	Time, LST	Percentage growth
159	0530-0630	1.5
	0630-0730	7.0
	0730-1030	47.1
	1030-1630	44.4
160	0530-0630	2.0
	0630-0730	6.0
	0730-0830	40.0
	0830-1030	32.5
	1030-1630	19.5
195	0630-0730	2.0
	0730-0830	40.0
	0830-0930	20.0
	0930-1530	38.0
205	0630-0730	5.0
	0730-1030	23.0
	1030-1630	72.0
216	0630-1030	64.0
	1030-1230	16.0
	1230-1530	20.0
226	0530-0730	4.5
	0730-0830	50.0
	0830-0930	18.0
	0930-1030	15.5
	1030-1630	12.0

TABLE V.- COMPARISON OF MEASURED TO MODELED OZONE MAXIMA

Day	Measured maximum ozone		Calculated maximum ozone		
	Concentration, ppb	Time of occurrence	Concentration, ppb	Time of occurrence	Change in concentration (modeled-measured), percent
159	124.	1330	145.	1530	+16.6
160	163.	1430	174.	1530	+7.01
195	151.	1530	151.	1630	0.
205	83.1	1330	94.5	1530	+13.7
216	108.	1630	121.	1630	+11.7
226	144.	1530	148.	1630	+3.12

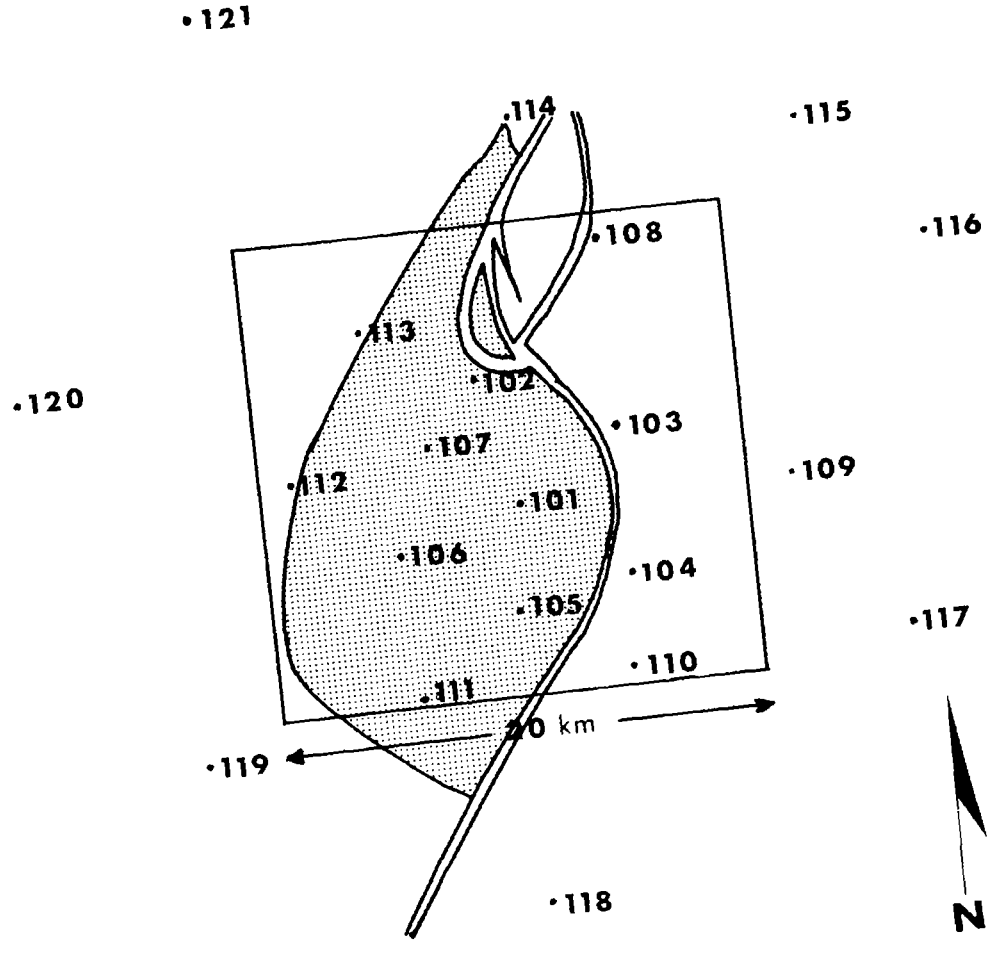

Figure 1.- Locations of RAM stations used to obtain RAPS data set. Shaded area represents urban St. Louis.

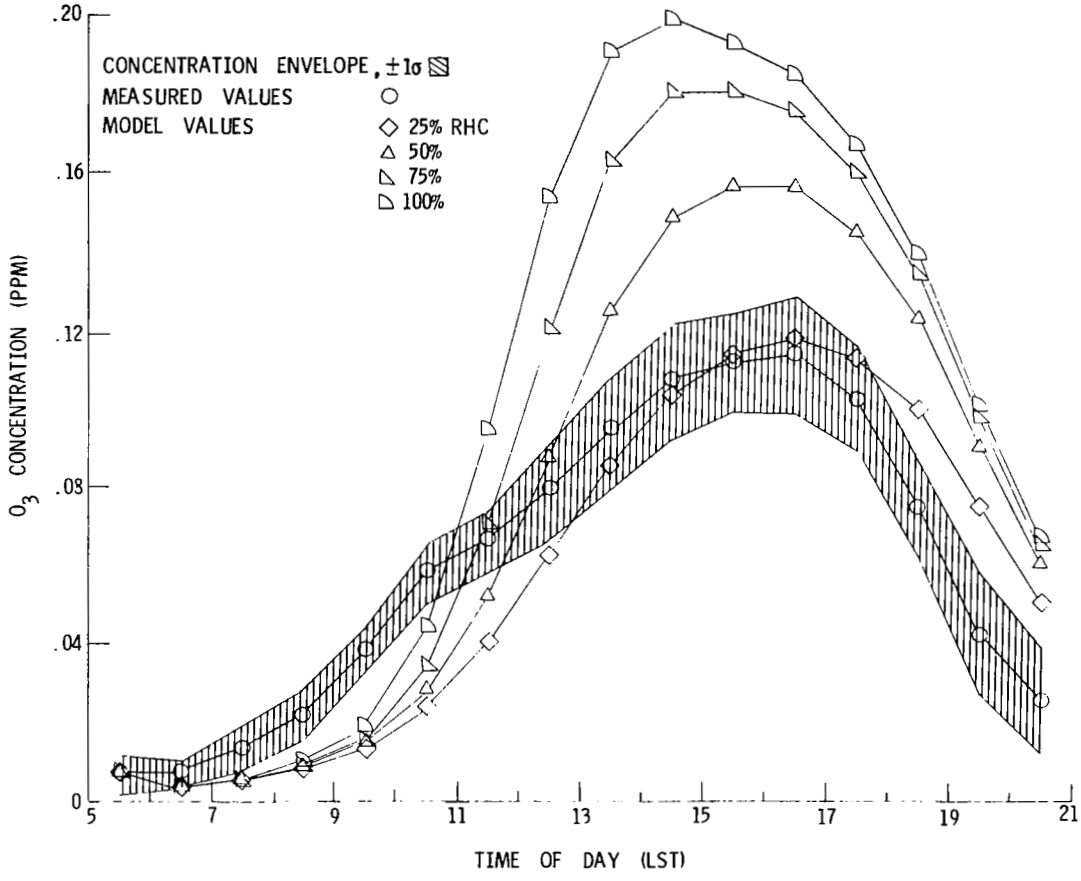

Figure 2.- Effect of varying total hydrocarbon partitioning coefficients on predicted diurnal ozone concentration in St. Louis for day 216. Coefficients represent various percentages of reactive hydrocarbon (RHC) levels in Los Angeles.

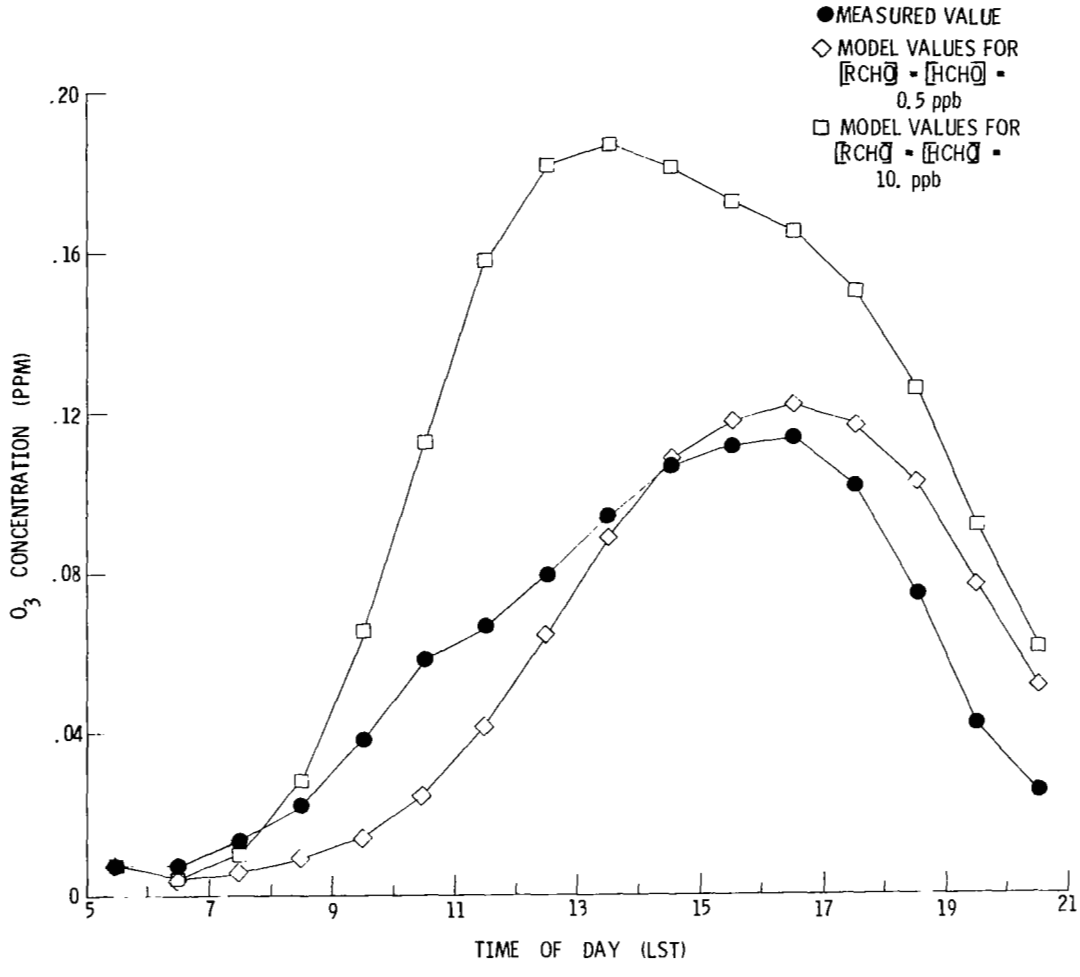

(a) Effect of changing concentrations of formaldehyde and other aldehydes to 10 ppb.

Figure 3.- Effect of changing concentrations of selected species concentrations on predicted diurnal concentration of ozone for day 216.

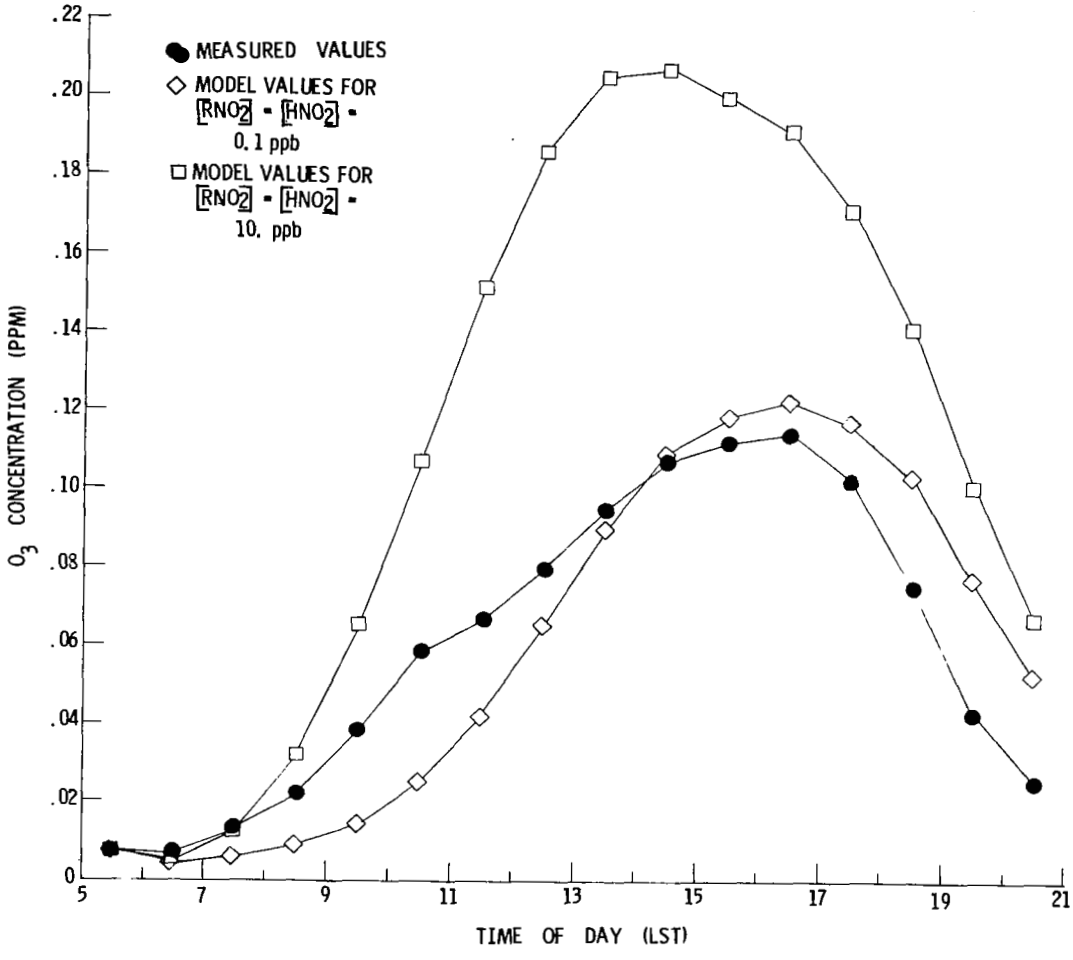

(b) Effect of changing concentrations of organic nitrates to 10 ppb and nitrous acid to 10 ppb.

Figure 3.- Concluded.

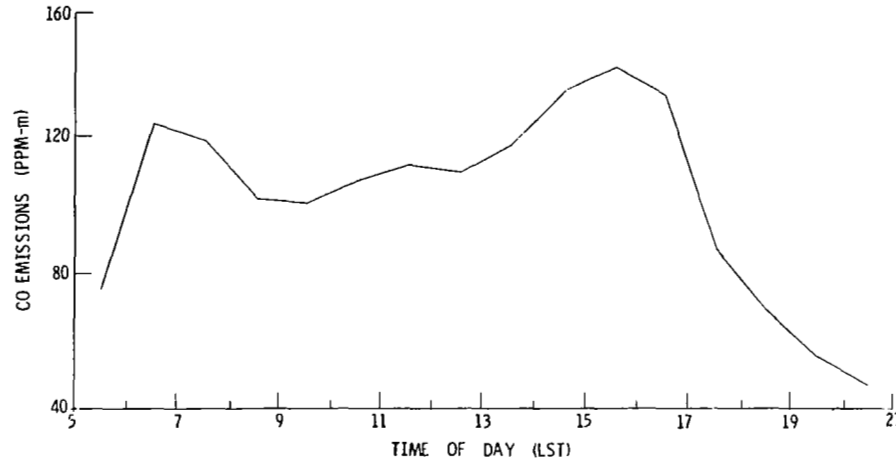

(a) CO.

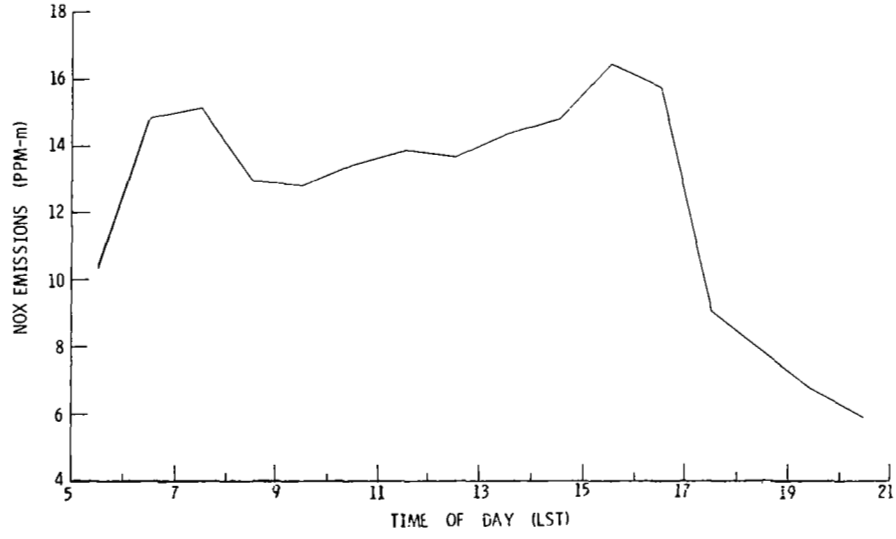

(b) NO_x.

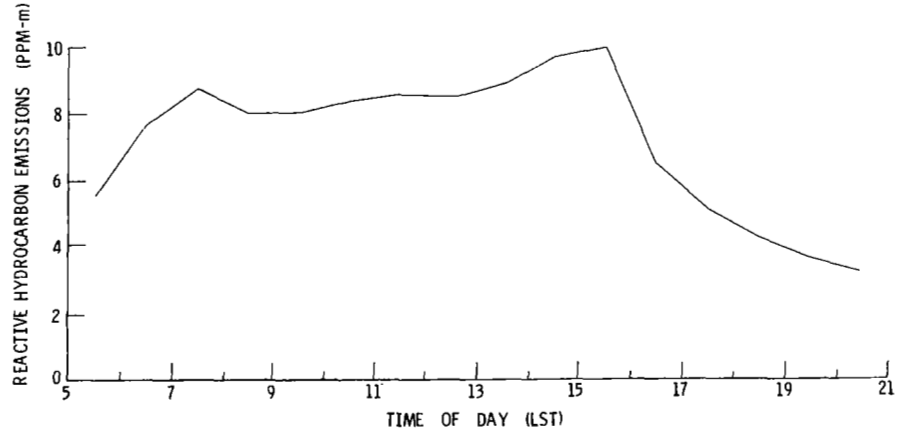

(c) Reactive hydrocarbons.

Figure 4.- Diurnal emissions inside cell for day 216.

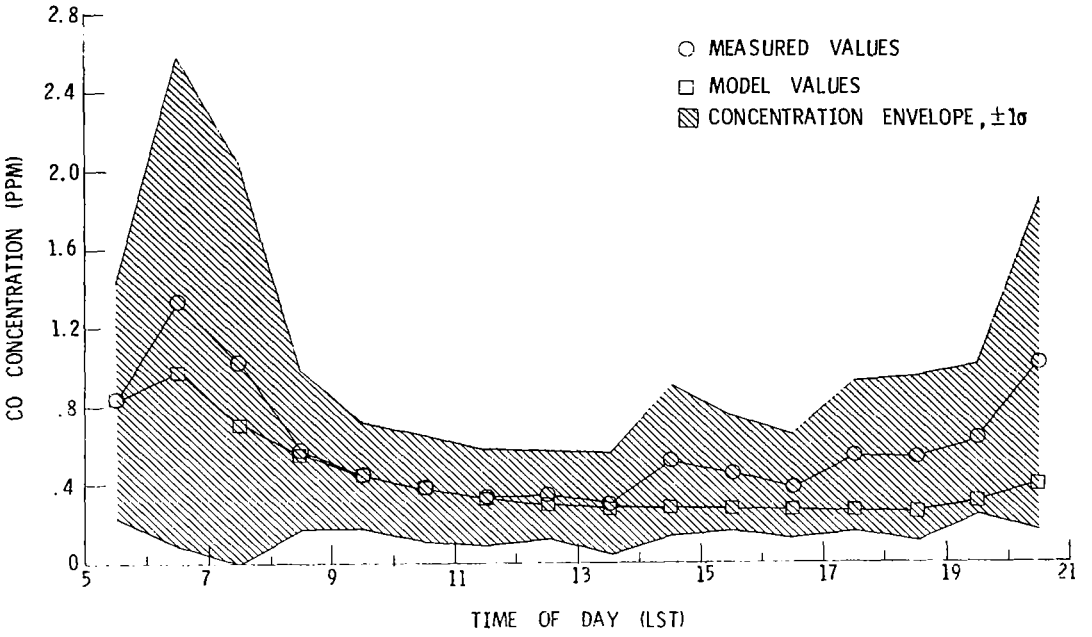

(a) CO.

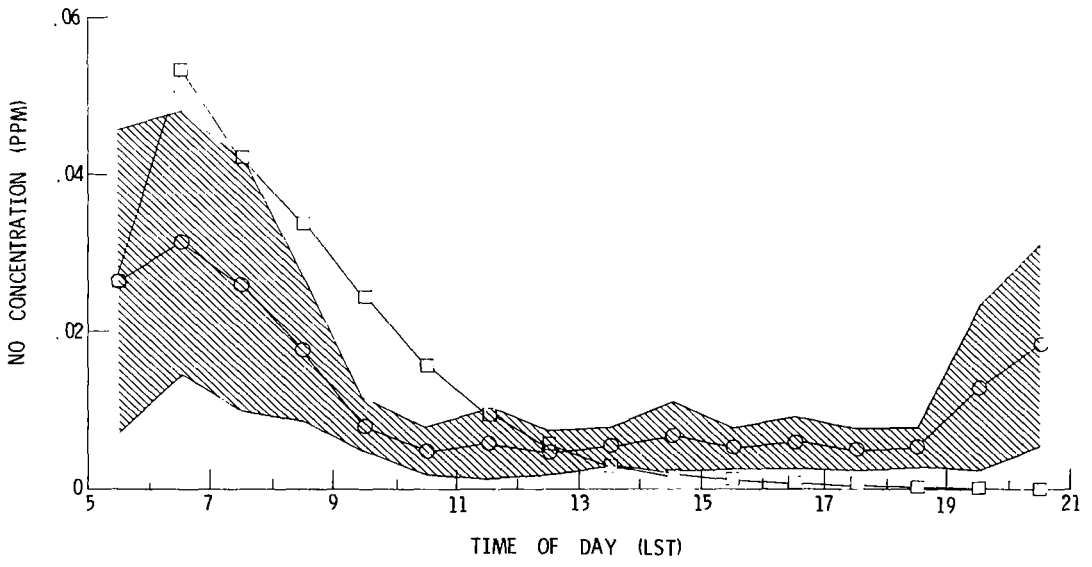

(b) NO.

Figure 5.- Hourly averaged measured and modeled species concentrations for day 216.

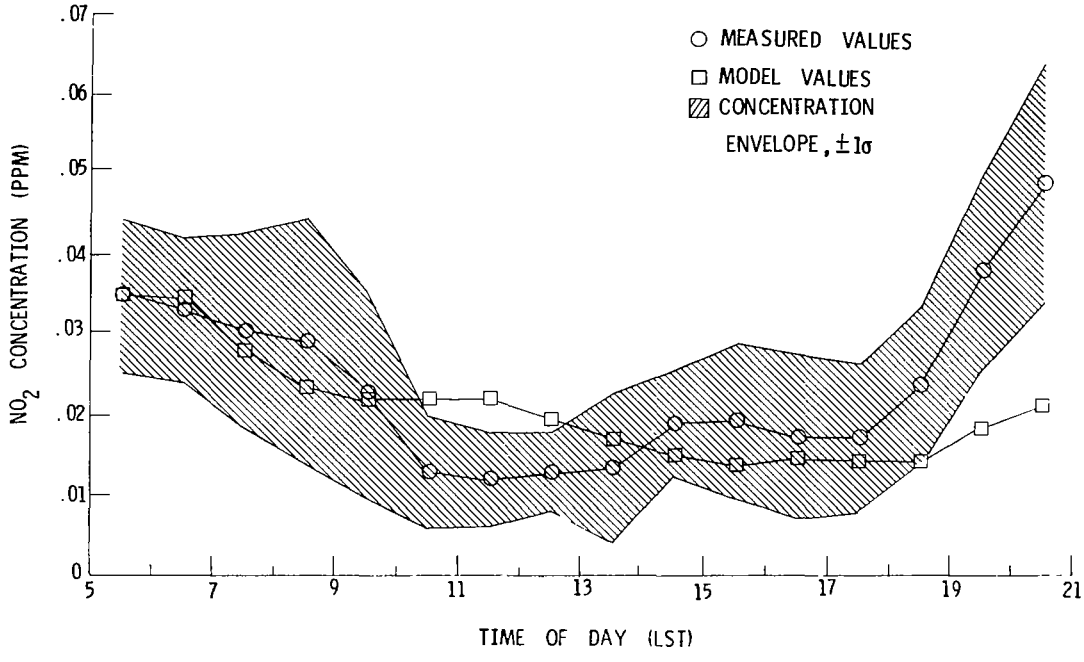

(c) NO_2.

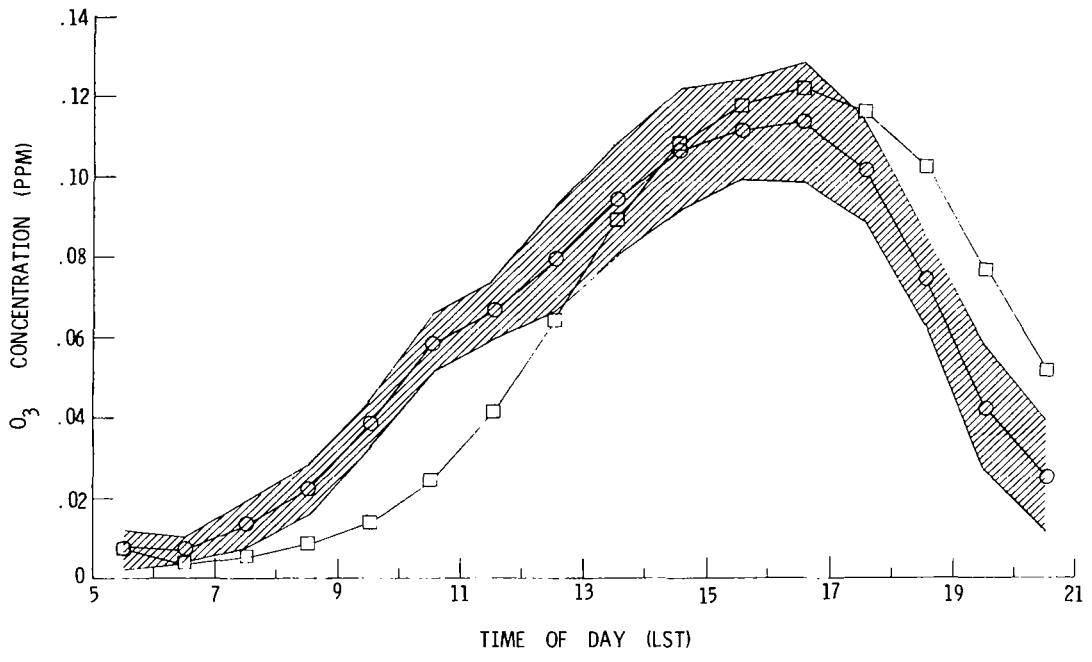

(d) O_3.

Figure 5.- Concluded.

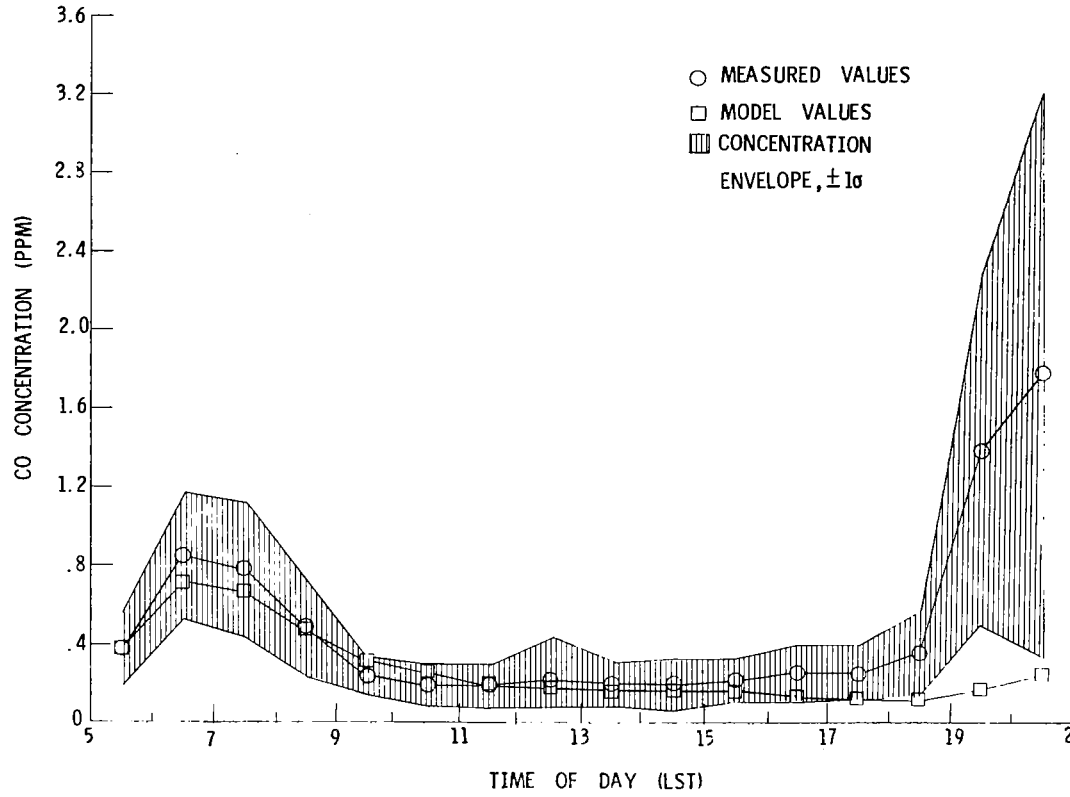

(a) CO.

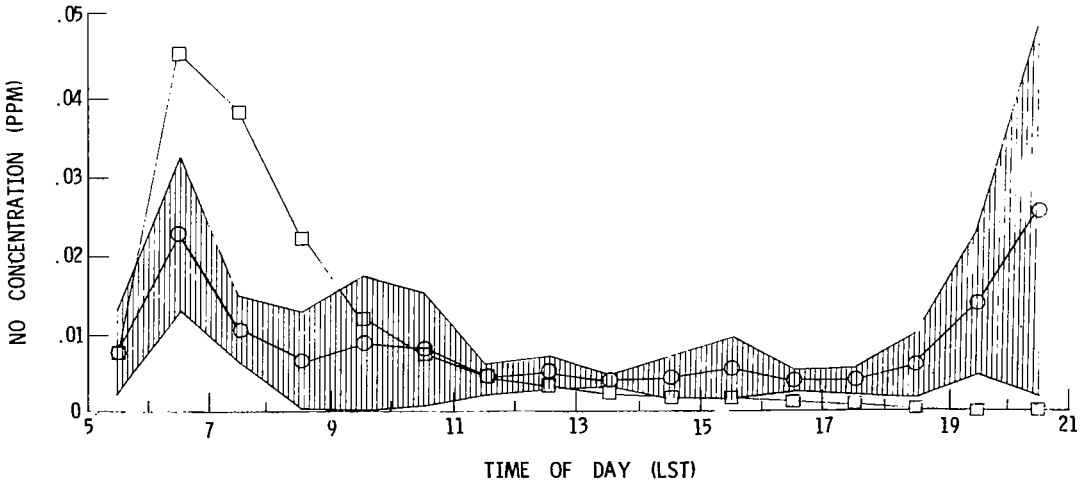

(b) NO.

Figure 6.- Hourly averaged measured and modeled species concentrations for day 205.

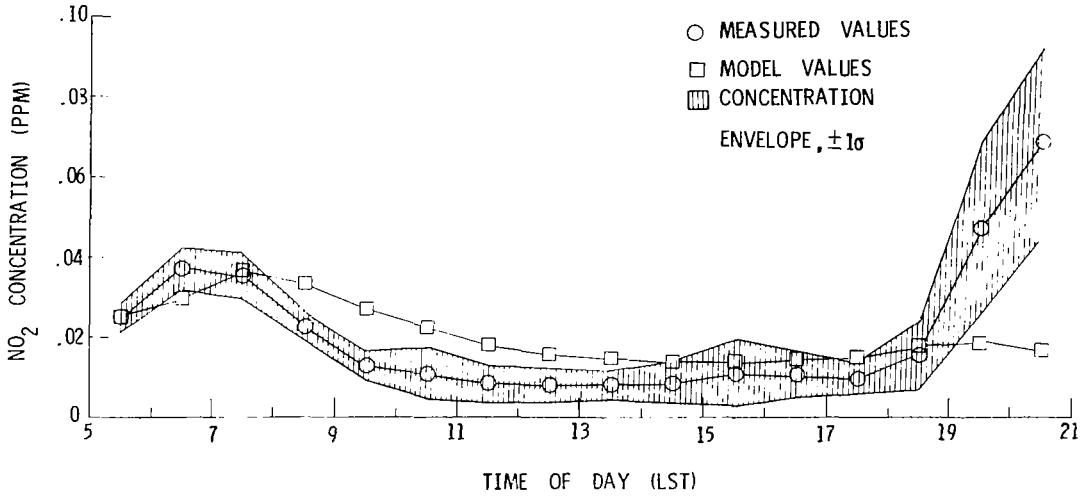

(c) NO_2.

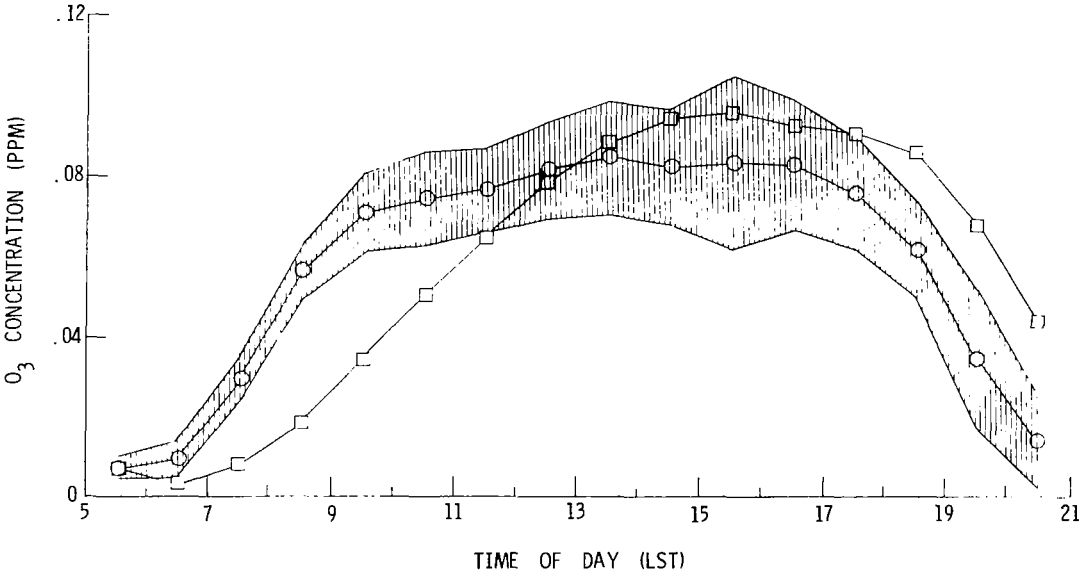

(d) O_3.

Figure 6.- Concluded.

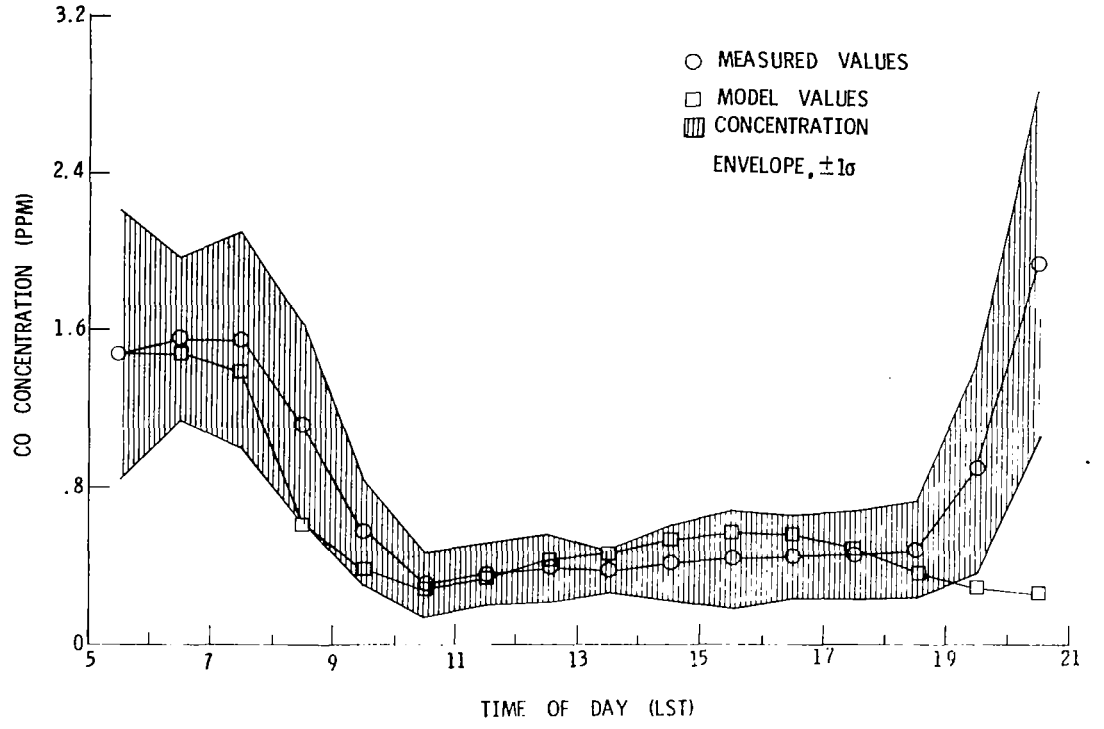

(a) CO.

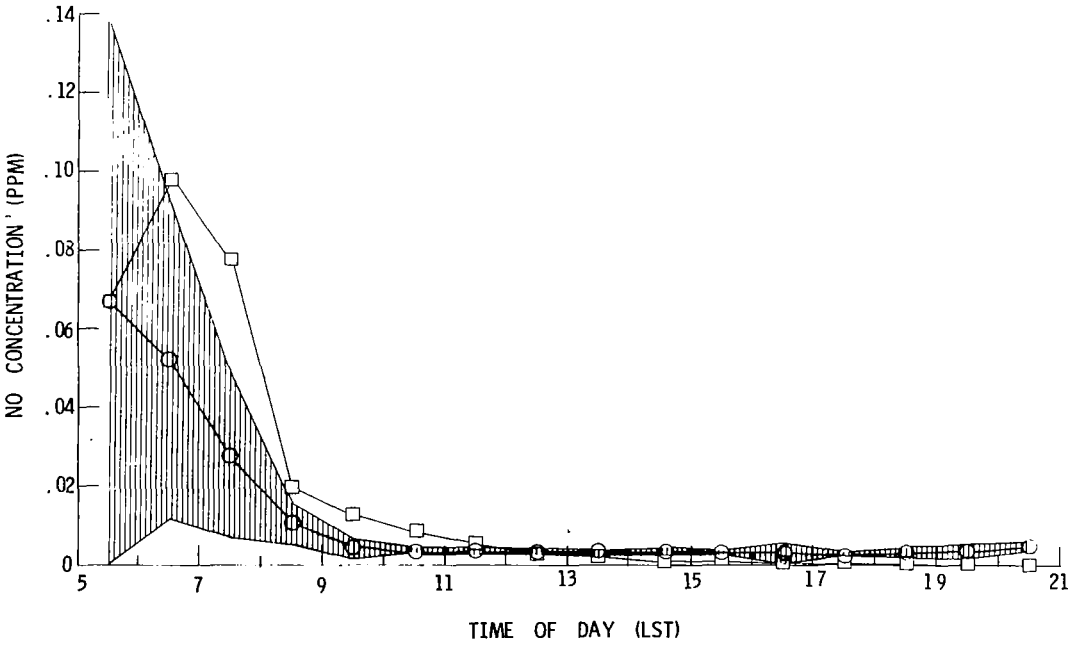

(b) NO.

Figure 7.- Hourly averaged measured and modeled species concentrations for day 160.

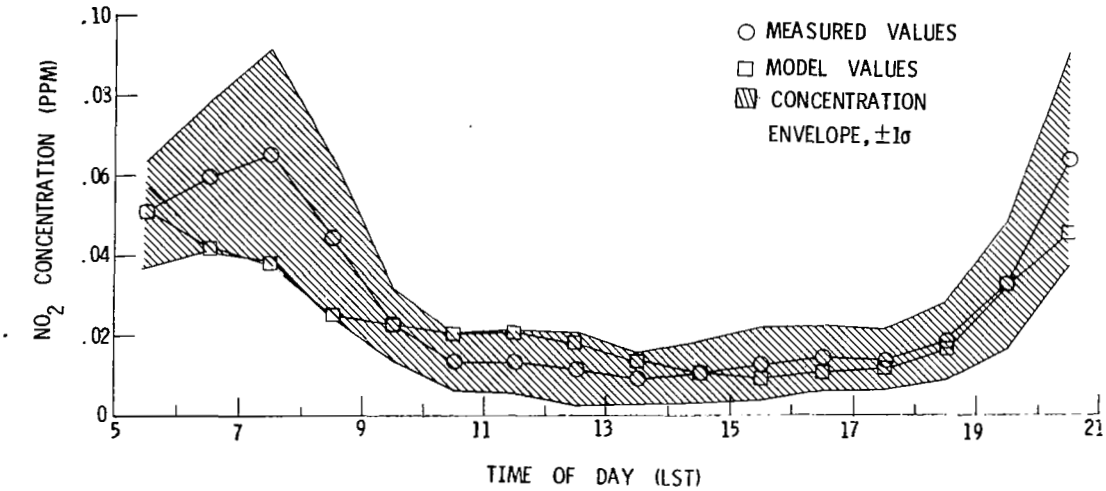

(c) NO_2.

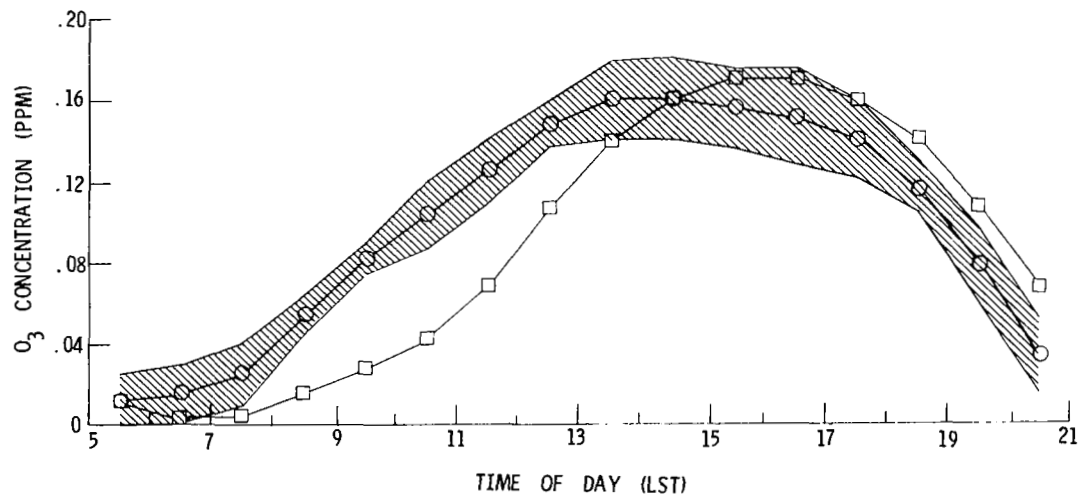

(d) O_3.

Figure 7.- Concluded.

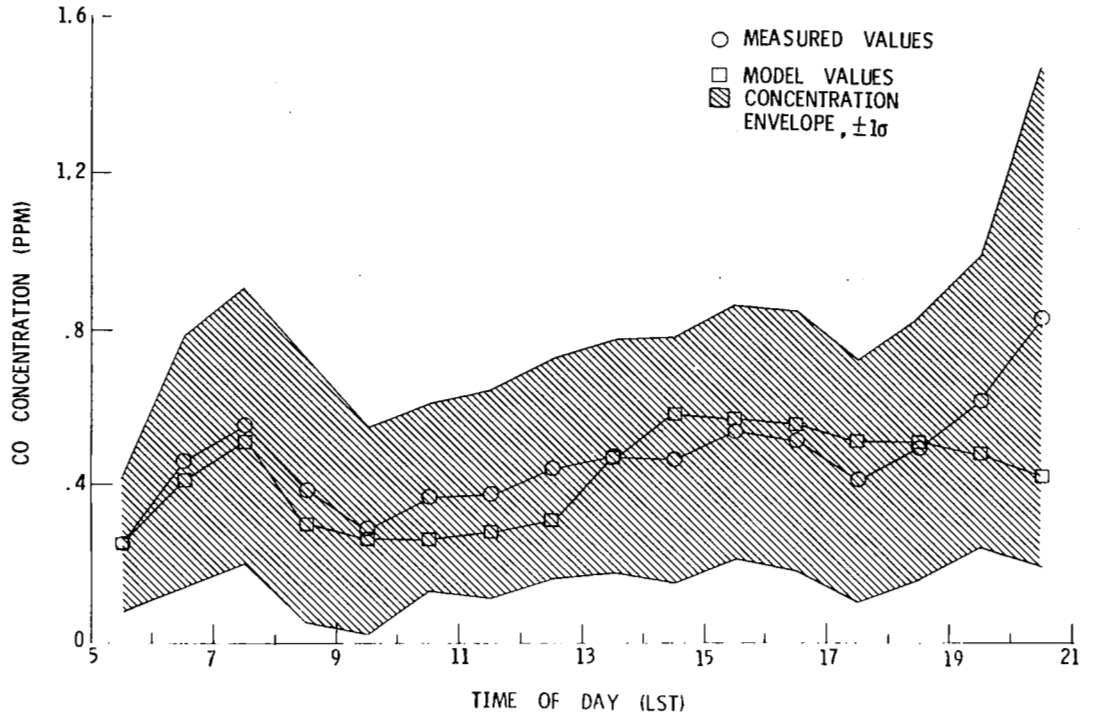

(a) CO.

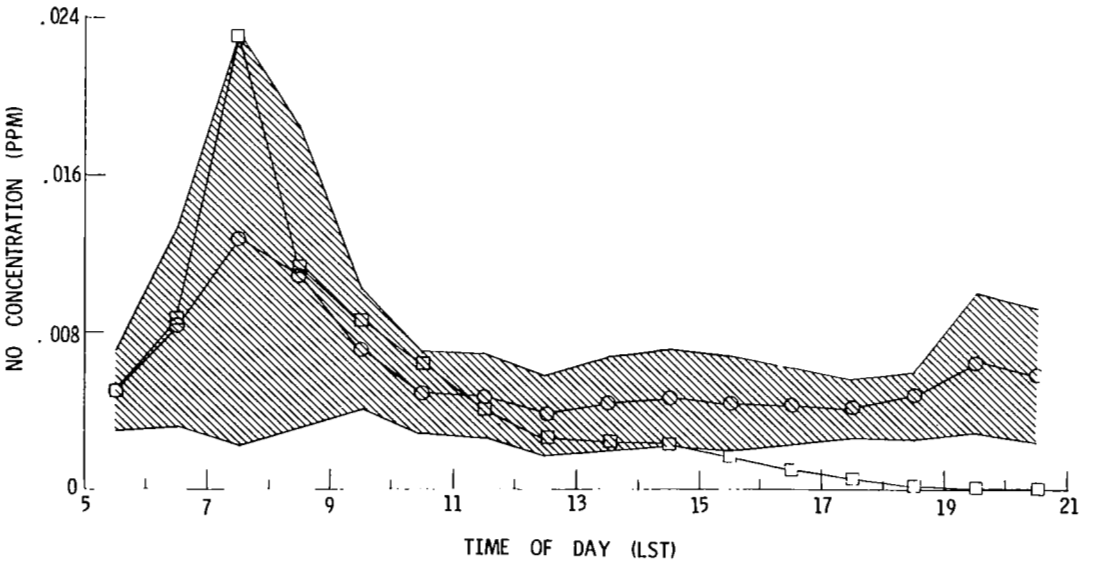

(b) NO.

Figure 8.- Hourly averaged measured and modeled species concentrations for day 195.

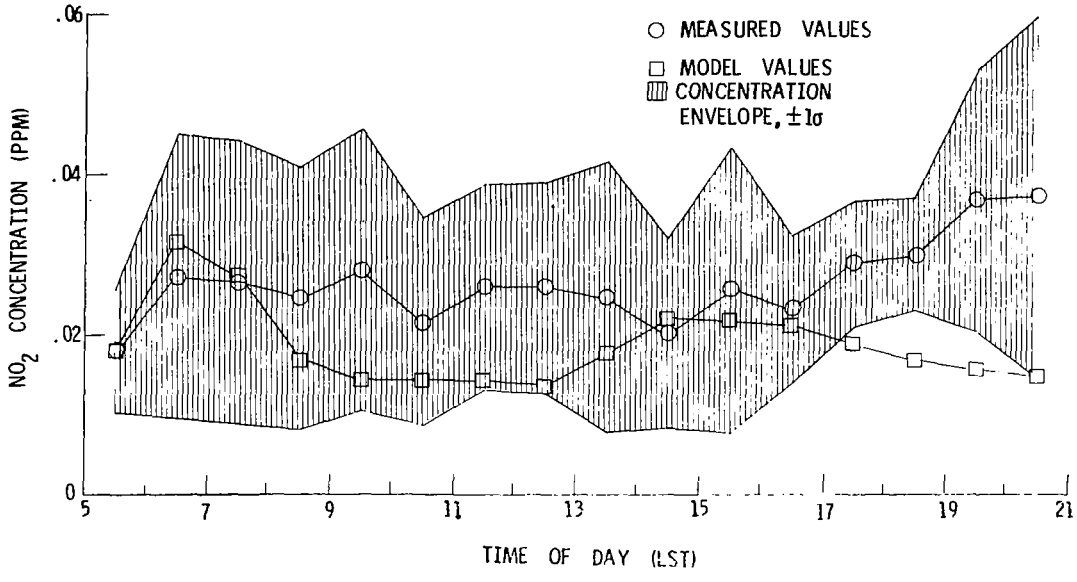

(c) NO_2.

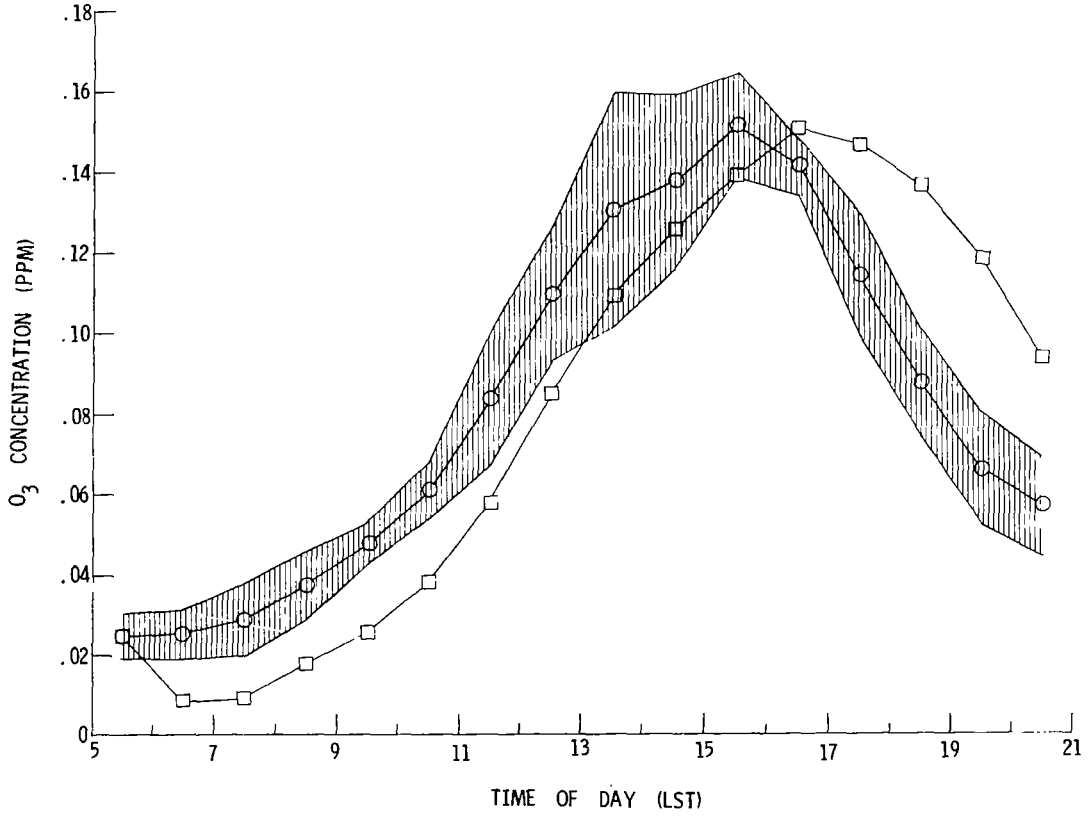

(d) O_3.

Figure 8.- Concluded.

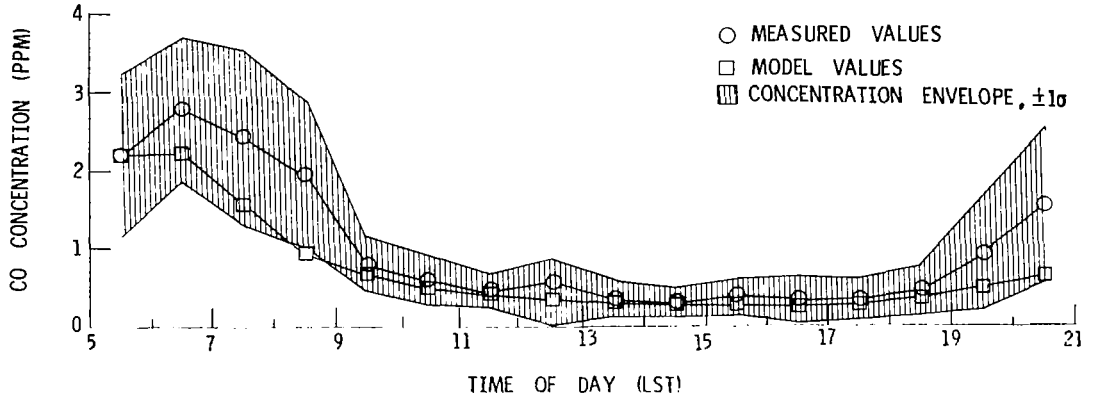

(a) CO.

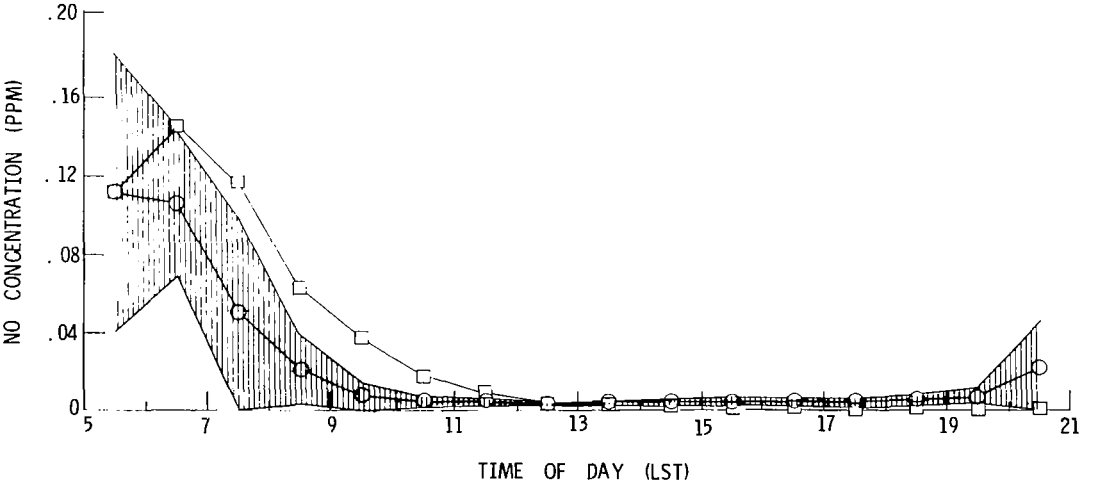

(b) NO.

Figure 9.- Hourly averaged measured and modeled species concentrations for day 159.

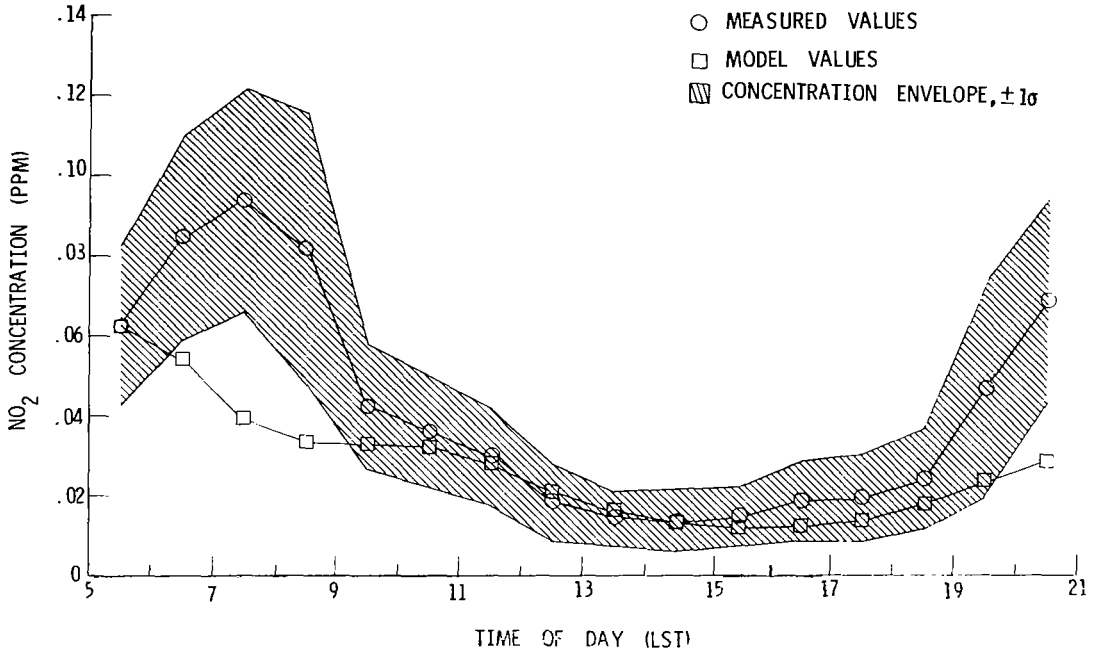

(c) NO_2.

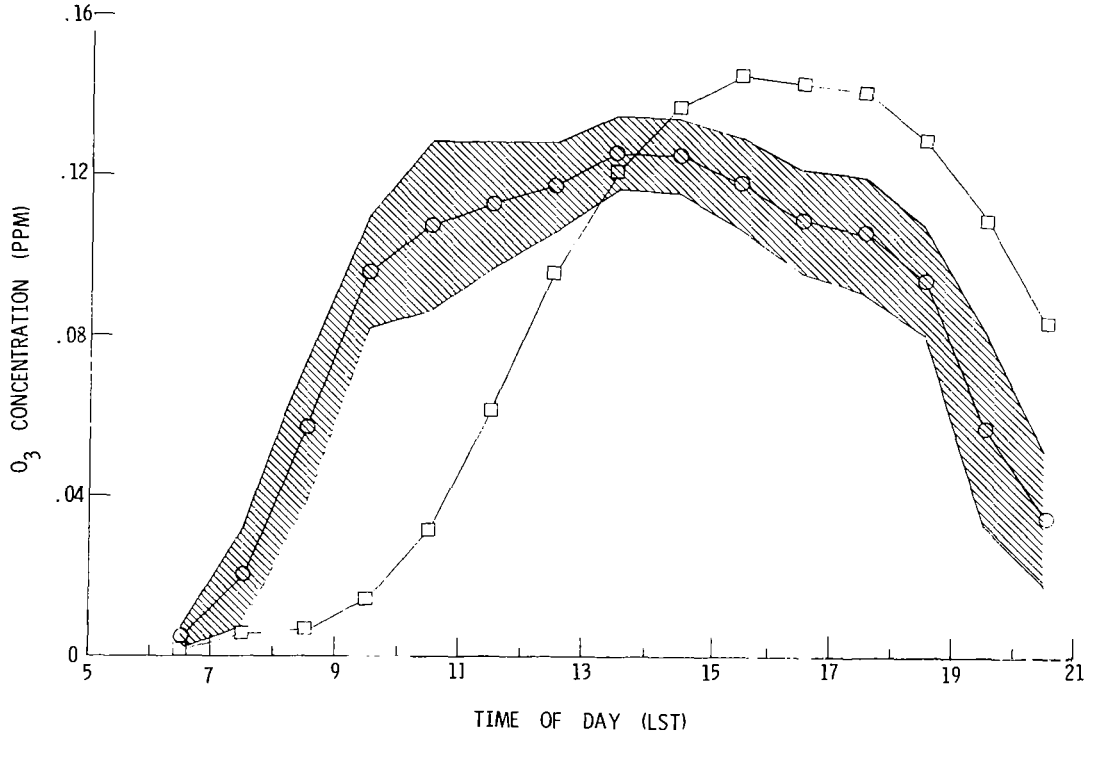

(d) O_3.

Figure 9.- Concluded.

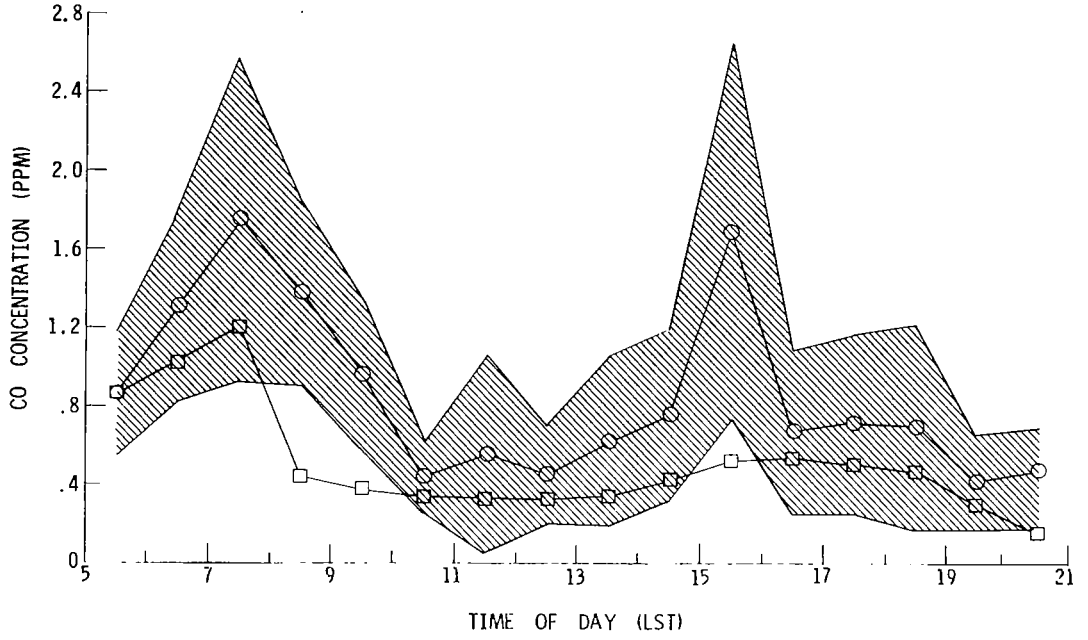

(a) CO.

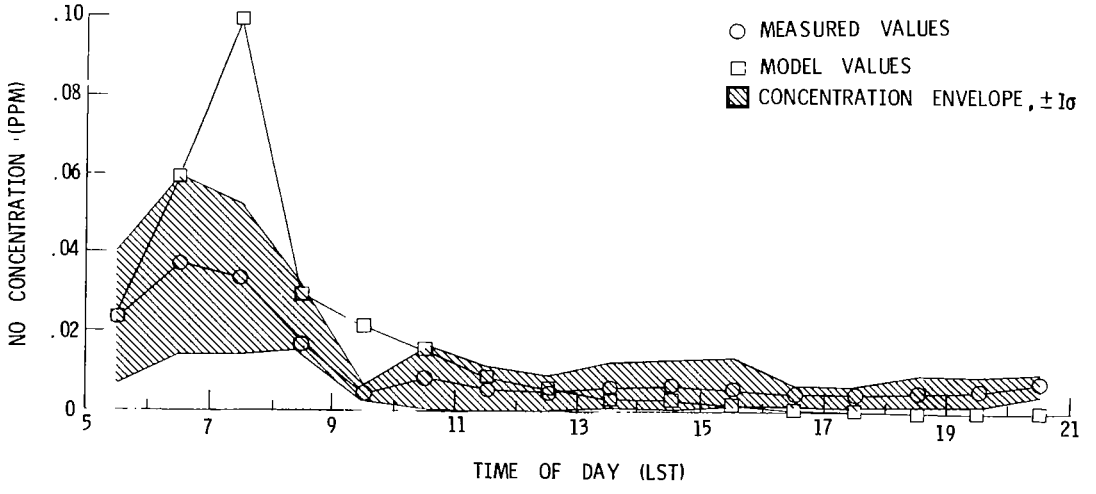

(b) NO.

Figure 10.- Hourly averaged measured and modeled species concentrations for day 226.

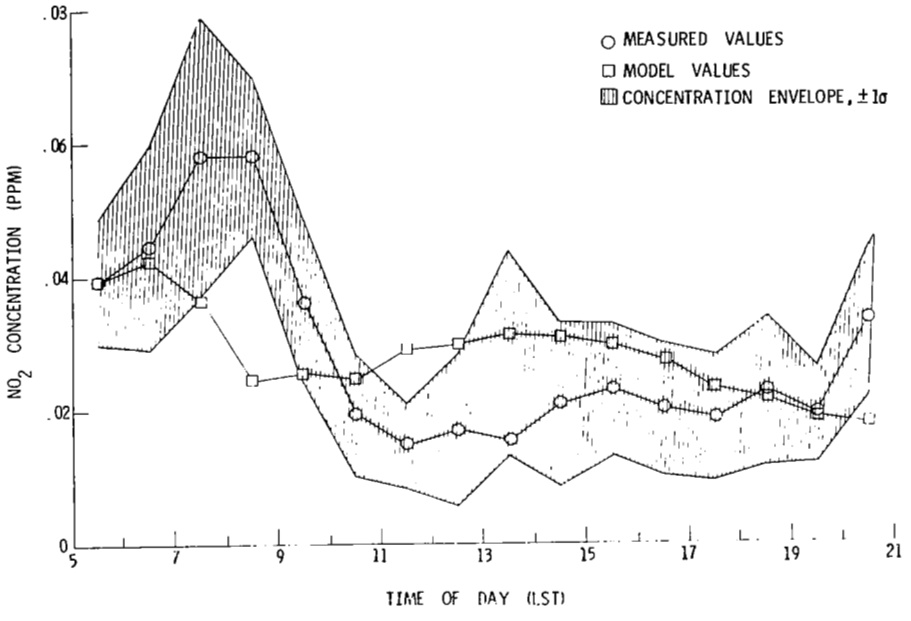

(c) NO_2.

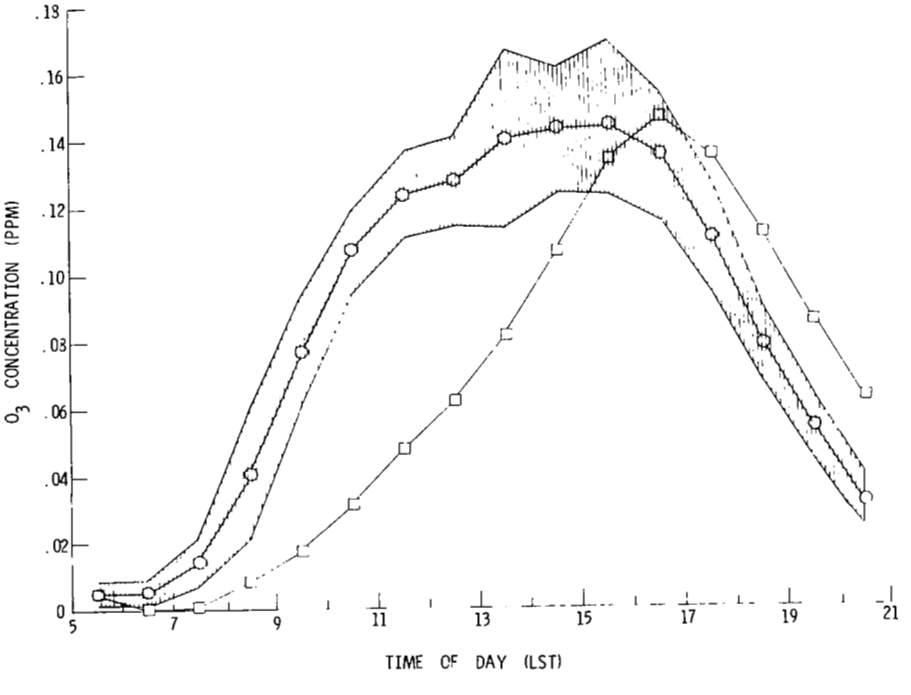

(d) O_3.

Figure 10.- Concluded.

1. Report No.	2. Government Accession No.	3. Recipient's Catalog No.
NASA TP-1843		

4. Title and Subtitle	5. Report Date
A DIAGNOSTIC MODEL FOR STUDYING DAYTIME URBAN AIR-QUALITY TRENDS	May 1981
	6. Performing Organization Code 146-20-10-30
7. Author(s) Dana A. Brewer, Ellis E. Remsberg, and Gerard E. Woodbury	8. Performing Organization Report No. L-14251
	10. Work Unit No.
9. Performing Organization Name and Address NASA Langley Research Center Hampton, VA 23665	11. Contract or Grant No.
	13. Type of Report and Period Covered Technical Paper
12. Sponsoring Agency Name and Address National Aeronautics and Space Administration Washington, DC 20546	14. Sponsoring Agency Code

15. Supplementary Notes

Dana A. Brewer: Joint Institute for Advancement of Flight Sciences, The George Washington University, Hampton, Virginia.
Ellis E. Remsberg and Gerard E. Woodbury: Langley Research Center.

16. Abstract

A single-cell Eulerian photochemical air-quality simulation model was developed and validated for selected days of the 1976 St. Louis Regional Air Pollution Study (RAPS) data sets; parameterizations of variables in the model and validation studies using the model are discussed. Good agreement was obtained between measured and modeled concentrations of NO, CO, and NO_2 for all days simulated. The maximum concentration of O_3 was also predicted well. Predicted species concentrations were relatively insensitive to small variations in CO and NO_x emissions and to the concentrations of species which are entrained as the mixed layer rises. Because of the rather small horizontal dimensions of the single cell (20 km by 20 km), predicted species concentrations were sensitive to the advection of upwind ozone and it precursors. Chemical reactions were dominated by the chemistry of reactive hydrocarbons. Significant changes in the predicted concentrations of O_3 were also obtained when photolytic reaction rates were scaled from theoretical to atmospheric values to reflect the attenuation of solar radiation by particulates and aerosols. The uses of additional types of data in the model formulation and validation procedures are discussed.

17. Key Words (Suggested by Author(s))	18. Distribution Statement
Air pollution Photochemical smog Urban modeling RAPS data set	Unclassified - Unlimited Subject Category 45

19. Security Classif. (of this report)	20. Security Classif. (of this page)	21. No. of Pages	22. Price
Unclassified	Unclassified	40	A03

For sale by the National Technical Information Service, Springfield, Virginia 22161

NASA-Langley, 1981